

1 **The Effect of Meteorological Conditions and Atmospheric Composition in the**
2 **Occurrence and Development of New Particle Formation (NPF) Events in**
3 **Europe**

4
5 **Dimitrios Bousiotis¹, James Brean¹, Francis Pope¹, Manuel Dall'Osto²**
6 **Xavier Querol³, Andres Alastuey³, Noemi Perez³, Tuukka Petäjä⁴**
7 **Andreas Massling⁵, Jacob Klenø Nøjgaard⁵, Claus Nørdrstrom⁵**
8 **Giorgos Kouvarakis⁶, Stergios Vratolis⁷, Konstantinos Eleftheriadis⁷**
9 **Jarkko V. Niemi⁸, Harri Portin⁸, Alfred Wiedensohler⁹, Kay Weinhöhl⁹, Maik Merkel⁹,**
10 **Thomas Tuch⁹ and Roy M. Harrison^{1a*}**

11
12 **¹Division of Environmental Health and Risk Management**
13 **School of Geography, Earth and Environmental Sciences**
14 **University of Birmingham, Edgbaston, Birmingham B15 2TT, United Kingdom**

15
16 **²Institute of Marine Sciences, Passeig Marítim de la Barceloneta, 37-49 E-08003**
17 **Barcelona, Spain**

18
19 **³Institute of Environmental Assessment and Water Research (IDAEA - CSIC)**
20 **08034, Barcelona, Spain**

21
22 **⁴Institute for Atmospheric and Earth System Research (INAR) / Physics, Faculty of Science**
23 **University of Helsinki, Finland**

24
25 **⁵Department for Environmental Science, Aarhus University, DK-400, Roskilde, Denmark**

26
27 **⁶Environmental Chemical Processes Laboratory (ECPL), Department of Chemistry, University of**
28 **Crete, 70013, Heraklion, Greece**

29
30 **⁷Environmental Radioactivity Laboratory, Institute of Nuclear and Radiological Science &**
31 **Technology, Energy & Safety, NCSR Demokritos, Athens, Greece**

32
33 **⁸Helsinki Region Environmental Services Authority (HSY),**
34 **FI-00066 HSY, Helsinki, Finland**

35
36 **⁹Leibniz Institute for Tropospheric Research (TROPOS),**
37 **Permoserstr. 15, 04318 Leipzig, Germany**

38
39 **^aAlso at: Department of Environmental Sciences / Center of Excellence in Environmental Studies,**
40 **King Abdulaziz University, PO Box 80203, Jeddah, 21589, Saudi Arabia**

42 **ABSTRACT**

43 Although new particle formation (NPF) events have been studied extensively for some decades, the
44 mechanisms that drive their occurrence and development are yet to be fully elucidated. Laboratory
45 studies have done much to elucidate the molecular processes involved in nucleation, but this
46 knowledge has yet to be conclusively linked to NPF events in the atmosphere. There is great
47 difficulty in successful application of the results from laboratory studies to real atmospheric
48 conditions, due to the diversity of atmospheric conditions and observations found, as NPF events
49 occur almost everywhere in the world without always following a clearly defined trend of
50 frequency, seasonality, atmospheric conditions or event development.

51

52 The present study seeks common features in nucleation events by applying a binned linear
53 regression over an extensive dataset from 16 sites of various types (combined dataset of 85 years
54 from rural and urban backgrounds as well as roadside sites) in Europe. At most sites, a clear
55 positive relation is found between the solar radiation intensity (up to $R^2 = 0.98$), temperature (up to
56 $R^2 = 0.98$) and atmospheric pressure (up to $R^2 = 0.97$) with the frequency of NPF events, while
57 relative humidity (RH) presents a negative relation (up to $R^2 = 0.95$) with NPF event frequency,
58 though exceptions were found among the sites for all the variables studied. Wind speed presents a
59 less consistent relationship which appears to be heavily affected by local conditions. While some
60 meteorological variables (such as the solar radiation intensity and RH) appear to have a crucial

61 effect on the occurrence and characteristics of NPF events, especially at rural sites, it appears that
62 their role becomes less marked when at higher average values.

63

64 The analysis of chemical composition data presents interesting results. Concentrations of almost all
65 chemical compounds studied (apart from O₃) and the Condensation Sink (CS) have a negative
66 relationship with NPF event frequency, though areas with higher average concentrations of SO₂ had
67 higher NPF event frequency. Particulate Organic Carbon (OC), Volatile Organic Compounds
68 (VOCs) and particulate phase sulphate consistently had a positive relation with the growth rate of
69 the newly formed particles. As with some meteorological variables, it appears that at increased
70 concentrations of pollutants or the CS, their influence upon NPF frequency is reduced.

71

72 1. INTRODUCTION

73 New Particle Formation (NPF) events are an important source of particles in the atmosphere
74 (Merikanto et al., 2009; Spracklen et al., 2010). These are known to have adverse effects on human
75 health (Schwartz et al., 1996; Politis et al., 2008; Kim, et al., 2015), as well as affecting the optical
76 and physical properties of the atmosphere (Makkonen et al., 2012; Seinfeld and Pandis, 2012).
77 While NPF events occur almost everywhere in the world (Dall'Osto et al., 2018; Kulmala et al.,
78 2017; O'Dowd et al., 2002; Wiedensohler et al., 2019; Chu et al., 2019; Kerminen et al., 2018),
79 with some exceptions reported in forest (Lee et al., 2016; Pillai et al., 2013; Rizzo et al., 2010) or
80 high-elevation sites (Bae et al., 2010; Hallar et al., 2016), great diversity is found in the atmospheric
81 conditions within which they take place. The many studies conducted have included many different
82 types of location (urban, traffic, regional background), around the world and differences were found
83 in both the seasonality and intensity of NPF events. This variability may be related to the mix of
84 conditions that are specific to each location, which obscures the general understanding of the
85 conditions that are favourable for the occurrence of NPF events (Berland et al., 2017; Bousiotis et
86 al., 2020). For example, solar radiation is considered as one of the most important factors in the
87 occurrence of NPF events (Kulmala and Kerminen, 2008; Kürten et al., 2016; Pikridas et al., 2015;
88 Salma et al., 2011), as it drives the photochemical reactions leading to the formation of sulphuric
89 acid (Petäjä et al., 2009; Cheung et al., 2013), which is frequently the main component of the
90 formation and growth of the initial clusters (Iida et al., 2008; Stolzenburg et al., 2020; Weber et al.,
91 1995). Nevertheless, in many cases NPF events do not occur in the seasons with the highest

92 insolation (Park et al., 2015; Vratolis et al., 2019). Similarly, uncertainty exists over the effect of
93 temperature (Yli-Juuti et al., 2020; Stolzenburg et al., 2018). Higher temperatures are considered
94 favourable for the growth of the newly formed particles as increased concentrations of both
95 Biogenic Volatile Organic Compounds (BVOCs) and Anthropogenic Volatile Organic Compounds
96 (AVOCs) (Yamada, 2013; Paasonen et al., 2013) and their oxidation products (Ehn et al., 2014)
97 support growth of the particles. On the other hand, the negative effect of increased temperature
98 upon the stability of molecular clusters should not be overlooked (Kürten et al., 2018; Zhang et al.,
99 2012). The former factor appears frequently be dominant, as higher growth rates are found in most
100 cases in the local summer (Nieminen et al., 2018), although the actual importance of those VOCs in
101 the occurrence of NPF events is still not fully elucidated, with oxidation mechanisms still under
102 intense research (Tröstl et al., 2016; Wang et al., 2020). The effect of other meteorological variables
103 is even more complex, with studies presenting mixed results on the effect of the wind speed and
104 atmospheric pressure. Extreme values of those variables may be favourable for the occurrence of
105 NPF events, as they are associated with increased mixing in the atmosphere, but at the same time
106 suppress nucleation due to increased dilution of precursors (Brines et al., 2015; Rímnáková et al.,
107 2011; Shen et al., 2018; Siakavaras et al., 2016), or favour it due to a reduced condensation sink
108 (CS).

109

110 The effect of atmospheric composition on NPF events is also a puzzle of mixed results. While the
111 negative effect of the increased CS on the occurrence of the events is widely accepted (Kalkavouras

112 et al., 2017 ; Kerminen et al., 2004; Wehner et al., 2007), cases are found when NPF events occur
113 on days with higher CS compared to average conditions (Größ et al., 2018; Kulmala et al., 2005).
114 Sulphur dioxide (SO₂), which is one of the most important contributors to many NPF pathways, in
115 most studies was found at lower concentrations on NPF event days compared to average conditions
116 (Alam et al., 2003; Bousiotis et al., 2019), although there are studies that have reported the opposite
117 (Woo et al., 2001; Charron et al., 2008). Additionally, in a combined study of NPF events in China,
118 events were found to be more probable under sulphur-rich conditions rather than sulphur-poor
119 (Jayaratne et al., 2017). Similar is the case with the BVOCs and AVOCs, which present great
120 variability depending the area studied (Dai et al., 2017), and their contribution in the growth of the
121 particles is not fully understood yet. Until recently, it was considered unlikely for NPF events, as
122 they are considered in the present study (deriving from secondary formation not associated with
123 traffic related processes such as dilution of the engine exhaust), to occur within the complex urban
124 environment due to the increased presence of compounds, mainly associated with combustion
125 processes, which would suppress the survival of the newly formed particles within this type of
126 environment (Kulmala et al., 2017). Despite this, NPF events were found to occur within even the
127 most polluted areas and sometimes with high formation and growth rates (Bousiotis et al., 2019;
128 Yao et al., 2018).

129

130 It is evident that while a general knowledge of the role of the meteorological and atmospheric
131 variables has been achieved, there is great uncertainty over the extent and variability of their effect

132 (and for some of them even the direction of an effect) in the mechanisms of NPF in real
133 atmospheric conditions, especially in the more complex urban environment (Harrison, 2017). The
134 present study, using an extensive dataset from 16 sites in six European countries, attempts to
135 elucidate the effect of several meteorological and atmospheric variables not only in general, but also
136 depending on the geographical region or type of environment. While studies with multiple sites
137 have been reported in the past (Dall'Osto et al., 2018; Kulmala et al., 2005; Rivas et al., 2020), to
138 the authors' knowledge this is the first study that focuses directly on the effect of these variables
139 upon the frequency of NPF events as well as the formation and growth rates of newly formed
140 particles in real atmospheric conditions.

141

142 **2. DATA AND METHODS**

143 **2.1 Site Description and Data Availability**

144 The present study uses a total of more than 85 years of hourly data from 16 sites from six countries
145 of Europe of various land usage and climates. It was considered very important that at least a rural
146 and an urban site would be available from each country to study the differences between the
147 different land usage on NPF events throughout Europe. The sites were chosen to cover the greatest
148 possible extent of the European continent, with sites from both northern, central and southern
149 Europe, as well as from western and eastern. The sites are located in the UK (London and Harwell),
150 Denmark (Copenhagen greater area), Germany (Leipzig greater area), Finland (Helsinki and
151 Hyytiälä), Spain (Barcelona and Montseny – a site in a mountainous area) and Greece (Athens and

152 Finokalia). Unfortunately, not all sites had available data for all the variables studied, which to an
153 extent may bias some of the results. An extended analysis of the typical and NPF event conditions,
154 seasonal variations and trends at these sites for the same period is found in other studies (Bousiotis
155 et al., 2019; 2020). A list of the available data and a brief description for each site is found in Table
156 1 (for the ease of reading the sites are named by the country of the site followed by the last two
157 letters which refer to the type of site, being RU for rural/regional background, UB for urban
158 background and RO for roadside site), while a map of the sites is found in Figure 1. For all the sites,
159 the data used in the present study are of either 1-hour resolution or less. Data with coarser resolution
160 were omitted for reliability.

161

162 Most of the data used in this analysis were also published in previous studies. The data from the UK
163 were published in Bousiotis et al., (2019; 2020), while parts of it were also published in Beddows et
164 al., (2015; 2019). The data for the German sites and parts of the data from UK, Denmark and
165 Finland were also published in von Bismarck et al., (2013; 2014; 2015). Parts of the measurements
166 for the Spanish sites were used in Carnerero et al., (2019) and Brines et al., (2015). The data for the
167 Greek rural background site were published in Kalivitis et al., (2019). Finally, the data for the Greek
168 urban background site were extracted from the European database (EBAS – ebas.nilu.no) and to the
169 authors' knowledge has not been used in previous studies. Additional data for some of the sites
170 were provided from their respective operators and were also not used in the past.

171

172 **2.2 Methods**

173 **2.2.1 NPF events selection**

174 NPF events were selected using the method proposed by Dal Maso et al (2005). An NPF event is
175 identified by the appearance of a new mode or particles in the nucleation mode (smaller than 20 nm
176 in diameter), which prevails for some hours and shows signs of growth. The events can then be
177 classified into classes I and II according to the level of certainty, while class I events can be further
178 classified to Ia and Ib. Events having both a clear formation of a new mode of particles in the
179 smallest size bins available (thus excluding possible advected events) as well as a distinct and
180 persistent growth of the new mode of particles for at least 3 hours were classified as Ia, while Ib
181 consists of rather clear events that fail though by at least one of the criteria set. Additionally, for the
182 roadside sites, a formation of particles in the nucleation mode accompanied by a significant increase
183 of the concentrations of pollutants was not considered as an NPF event, as it may be associated with
184 mechanisms other than the secondary formation. In the present study, only the events of class Ia
185 were considered with the additional criterion of at least 1 nm h^{-1} growth for at least 3 hours. As the
186 available SMPS datasets for the sites in the U.K. are for particles of diameter greater than 16 nm,
187 additional criteria were set to ensure the correct extraction of NPF events, including the variations
188 of the particle number concentrations from a Condensation Particle Counter (CPC – measuring
189 particles with diameter from 7nm), as well as of the concentrations of gaseous pollutants and
190 aerosol constituents (please refer to the Methods section in Bousiotis et al., 2019).

191

192 **2.2.2 Calculation of condensation sink, growth rate, formation rate, and NPF event**
193 **frequency**

194 The condensation sink (CS) is calculated according to the method proposed by Kulmala et al.,
195 (2001) as:

196

$$197 \quad CS = 4\pi D_{vap} \sum \beta_M r N \quad (1)$$

198

199 where r and N is the radius and number concentration of the particles respectively and D_{vap} is the
200 diffusion coefficient calculated as (Poling et al., 2001):

201

$$202 \quad D_{vap} = 0.00143 \cdot T^{1.75} \frac{\sqrt{M_{air}^{-1} + M_{vap}^{-1}}}{P \left(D_{x,air}^{\frac{1}{3}} + D_{x,vap}^{\frac{1}{3}} \right)^2} \quad (2)$$

203

204 for $T = 293$ K and $P = 1013.25$ mbar. M and D_x are the molar mass and diffusion volume for air and
205 sulphuric acid. β_M is the Fuchs correction factor calculated as (Fuchs and Sutugin, 1971):

206

$$207 \quad \beta_M = \frac{1 + K_n}{1 + \left(\frac{4}{3a} + 0.377 \right) K_n + \frac{4}{3a} K_n^2} \quad (3)$$

208

209 where K_n is the Knudsen number, calculated as $K_n = 2\lambda_m/d_p$ where λ_m is the mean free path of the
210 gas. It should be noted that due to the lack of sufficient chemical composition data for a number of
211 sites, the CS calculated is not corrected for hygroscopic growth. As a result, the values for CS and
212 the results associated to it presented in this work, may be biased between the sites studied due to the
213 great differences in the conditions between them.

214

215 Growth rate (GR) is calculated as (Kulmala et al., 2012):

216

$$217 \quad GR = \frac{D_{P_2} - D_{P_1}}{t_2 - t_1} \quad (4)$$

218

219 for the size range between the minimum available particle diameter up to 30 nm (50 nm for the UK
220 sites due to the higher minimum particle size available). The time window used for the calculation
221 of the growth rate was from the start of the event until a) growth stopped, b) GMD reached the
222 upper limit set or c) the day ended.

223

224 The formation rate J was calculated using the method proposed by (Kulmala et al., 2012) as:

225

$$226 \quad J_{d_p} = \frac{dN_{d_p}}{dt} + \text{Coag}S_{d_p} \times N_{d_p} + \frac{GR}{\Delta d_p} \times N_{d_p} + S_{\text{losses}} \quad (5)$$

227

228 where CoagS_{d_p} is the coagulation rate of particles of diameter d_p , calculated as (Kerminen et al.,
229 2001):

230

$$231 \quad \text{CoagS}_{d_p} = \int K(d_p, d'_p) n(d'_p) dd'_p \cong \sum_{d'_p=d_p}^{d'_p=\max} K(d_p, d'_p) N_{d_p} \quad (6)$$

232

233 $K(d_p, d'_p)$ is the coagulation coefficient of particles with diameters d_p and d'_p , while S_{losses} accounts
234 for additional loss terms (i.e. chamber wall losses), which are not applicable in the present study.

235 For the present study, the formation rate of particles of diameter of 10 nm was calculated for

236 uniformity (16 nm for the UK sites), though most sites had data for particle sizes below 10 nm.

237

238 The NPF frequency was calculated by the number of NPF event days divided by the number of days

239 with available data in the given group (full dataset or temporal, variable ranges etc.). The results

240 presented in this study were normalised according to the data availability, as:

241

$$242 \quad NPF_{\text{frequency}} = \frac{N_{\text{NPF event days for group of days } X}}{N_{\text{days with available data for group of days } X}} \quad (7)$$

243 Finally, the p-values reported in the analysis derive from the ANOVA one-way test. As the

244 normality of the variables is required for such an analysis, the Shapiro-Wilk test was used to assess

245 the normality and the vast majority of the variables were found to have $p > 0.05$ and thus were

246 considered as normal. This is probably due to the removal of the extreme values (as mentioned in
247 section 2.2.3, for the calculations 90% of each dataset was kept removing the extremely high and/or
248 low values and the possible outliers included in them). While this was not done to promote the
249 normality of the populations but to reduce the bias from extreme values, it indirectly assisted in
250 making the distributions normal. For the few remaining (e.g. the growth rates associated with SO₂
251 concentrations for UKRO) for which normality was not present, the square root of the values of the
252 variable were considered to achieve normality and proceed to the ANOVA test.

253

254 **2.2.3 Calculation of the gradient and intercept for the variables used**

255 Due to the large datasets available and the great spread of the values, a direct comparison between a
256 given variable and any of the characteristics associated with NPF events (NPF frequency, growth
257 rate and formation rate) always provided results with low statistical significance. As a result, an
258 alternative method which can provide a reliable result without the dispersion of the large datasets
259 was used in the present study, to investigate the relationships between the variables which are
260 considered to be associated with the NPF events. For this, a timeframe which is more directly
261 associated with the NPF events typically observed in the mid-latitudes was chosen. For NPF
262 frequency and GR the timeframe between 05:00 to 17:00 Local Time (LT) was chosen, which is
263 considered the time when the vast majority of NPF events take place and further develop with the
264 growth of the particles. For the formation rate a smaller timeframe was chosen, 09:00 to 15:00 LT
265 which is ± 3 hours from the time of the maximum formation rate found for almost all sites (12:00

266 LT). This was done to exclude as far as possible the effect of the morning rush at the roadside sites,
267 as well as only to include the time window when the formation rate is mostly relevant to NPF
268 events (negative values that are more probable outside this timeframe and are not associated with
269 the formation of the particles would bias the results).

270

271 For the CS the timeframe 05:00 to 10:00 LT was chosen. This was done to avoid including the
272 direct effect of the NPF events (the contribution of newly formed particles to CS), as well as to
273 provide results for the conditions which either promote or suppress the characteristics studied,
274 which specifically for the CS are more important before the start of the events. The extreme values
275 (very high or very low) which bias the results only carrying a very small piece (forming bins of very
276 small size) of information were then removed, though 90% of the available data was used for all the
277 variables. The remaining data was separated into smaller bins and a minimum of 10 bins was
278 required for each variable (for example if the difference between the minimum and the maximum
279 relative humidity (RH) is 70%, then 14 bins each with a range of 5% were formed). The variables of
280 interest were then averaged for each bin and plotted, and a linear relation was considered for each
281 one of them. While it is evident that not all relationships are linear, the specific type was chosen in
282 the present analysis for all the variables studied. This was done because the aim was to elucidate the
283 general positive or negative effect of the variables studied. Furthermore, the effect of many
284 variables appears to vary between sites with great differences (either geographical or type of land

285 use) and the choice of a single method to describe these relationships ensures the uniformity of the
286 results, as it appears to better describe them in most cases.

287

288 The gradient of these linear relations (a_N , a_G and a_J for NPF frequency, growth rate and formation
289 rate J_{10} accordingly) found in this analysis should be used with great caution as apart from the
290 atmospheric conditions (local and meteorological as well as atmospheric composition) it is also
291 affected by the variable in question (e.g. a greater NPF frequency will provide a greater gradient),
292 resulting in giving the same trend for all the atmospheric variables tested; the sites with the higher
293 values of these variables (NPF frequency and formation rate) always had greater gradient values
294 and vice versa. In order to remove the effect of the variable in question (NPF frequency or
295 formation rate – growth rate will provide an unreliable result as it is calculated in a different range
296 for each site due to the lower available size of particles), the gradients were normalised by dividing
297 them by their respective variable (e.g. divide the gradient of the NPF frequency with the NPF
298 frequency), providing with a new normalised slope (a_N^* for NPF frequency or a_J^* for the formation
299 rate) that will have no significance other than its absolute value, which can be used for direct
300 comparisons:

301
$$a_N^* = \frac{a_N}{\text{NPF \%}}$$

302 Where a_N is the gradient of the relation between the given variable and NPF frequency (NPF %)

303

$$a_J^* = \frac{a_J}{J_{10}}$$

304
305 Where a_J is the gradient of the relation between the given variable and the formation rate of 10 nm
306 particles J_{10} (J_{16} for the UK sites).

307

308 **3. RESULTS**

309 In this study NPF events are generally observed as particles grow from a smaller size (typically 3-
310 16 nm depending on the size detection limit of instruments used) to 30 nm or larger. They therefore
311 reflect the result both of nucleation, which creates new particles of 1-2 nm (not detected with the
312 instruments used in this study), and growth to larger sizes. In analysing NPF events, we therefore
313 consider three diagnostic features:

- 314 • the frequency of events occurring (i.e. days with an event divided by total days with relevant
315 data, depending on the variable and range studied), As only class Ia events were only considered,
316 it is expected that the frequency of the events calculated should be lower than the expected one
317 if all types of events were included. This could result in values up to one third of those anticipated
318 if all types of events were considered. For the extent of this variation please refer to Bousiotis et
319 al., (2019; 2020) in which there is an extended analysis of the NPF events for each site, including
320 the special cases of NPF events that do not comply for the criteria set for class Ia.
- 321 • the rate of particle formation at a given size (J_{10} in this case), which was found to have unclear
322 seasonal trends among the sites and was higher for urban sites compared to rural in most cases
323 (Bousiotis, 2019; 2020)

324 • the growth rate of particles from the lower measurement limit to 30 nm (or 50 nm for the UK
325 sites), which was found to be greater during summer months for most of the sites, also studied in
326 the aforementioned works.

327

328 From the analysis of the extended dataset a total of 1952 NPF events were extracted and studied.

329 The NPF frequency, growth and formation rate for each site is found in Table 2. The seasonal

330 variation of NPF events is found in Figure S14.

331

332 **3.1 Meteorological Conditions**

333 The gradients, coefficients of determination (R^2 – the relationships found are characterised as weak

334 for $R^2 < 0.50$, strong for $0.50 < R^2 < 0.75$ and very strong for $R^2 > 0.75$) and the p-values from the

335 analysis of the meteorological variables, as well as the average conditions of these variables are

336 found in Table 3. The results for each site and variable are found in figures S1 – S5.

337

338 **3.1.1 Solar radiation intensity**

339 As mentioned earlier, solar radiation intensity is considered to be one of the most important

340 variables in NPF occurrence, as it contributes to the production of H_2SO_4 which is a main

341 component of the initial clusters and participates in the early growth of the newly formed particles.

342 Hidy et al. (1994) reported up to six times higher SO_2 oxidation rates into H_2SO_4 in typical summer

343 conditions compared to winter. For almost all sites this relation is confirmed with very strong

344 correlations ($R^2 > 0.75$) between the intensity of solar radiation and the frequency for NPF events to
345 occur. The relationship between the solar radiation and NPF frequency was positive at all sites and
346 only three sites (FINUB, SPARU and GREUB) presented weak correlations ($R^2 < 0.40$). Weaker
347 correlations were found for the southern European sites, which might be associated with the higher
348 averages for solar radiation intensity, or the interference of other processes (such as coinciding with
349 increased CS by recirculation of air masses (Carnerero et al., 2019)), possibly making it less of an
350 important factor for these areas.

351

352 The relationship of solar radiation with the growth rate was weaker in all cases and did not present a
353 clear trend. Only some rural background sites (GERRU, FINRU and GRERU) presented a strong
354 correlation ($R^2 > 0.50$). The relationship found in most cases was positive apart from two roadside
355 sites (GERRO and UKRO) and two urban background sites (GREUB and UKUB), though due to
356 the low $R^2 (< 0.10)$ these results cannot be considered with confidence. It seems though that the
357 solar radiation intensity is probably a more important factor at background sites rather than at
358 roadside sites, where possibly local conditions (such as local emissions) are more important (Olin et
359 al, 2020). Finally, the formation rate has a positive relationship with the solar radiation intensity,
360 with relatively strong correlations in most areas ($R^2 > 0.50$). The correlations were stronger at the
361 rural background sites compared to the roadside sites, which further underlines the increased
362 importance of this factor at this type of site. A negative relationship between the solar radiation
363 intensity and the formation rate was found at the GRERU site but the R^2 is very low ($R^2 = 0.05$).

364 Plotting the normalised gradients for NPF event frequency a_N^* with the average solar radiation
365 intensity at each site (Figure 2) a negative relationship is found ($R^2 = 0.62$), with the southern areas
366 (those with higher average solar intensity) having smaller a_N^* compared to those in higher latitudes
367 (and thus with a lower average solar radiation). This may indicate that while solar radiation is a
368 deciding factor in the occurrence of an NPF event, when in greater intensity its role becomes
369 relatively less important, a finding that was also implied by Wonaschütz et al. (2015). Additionally,
370 the a_I^* was found to be higher at all rural sites compared to their respective roadside sites (and
371 urban background sites for all but the Greek and German ones), making it a more important factor
372 at this type of site (Figure 3).

373

374 **3.1.2 Relative humidity**

375 Relative humidity is considered to have a negative effect on the occurrence of NPF events (Jeong et
376 al., 2010; Hamed et al., 2011; Park et al., 2015; Dada et al., 2017; Li et al., 2019). While water in
377 the atmosphere is one of the main compounds needed for the formation of the initial clusters either
378 on the binary or ternary nucleation theory (Henschel et al., 2016; Korhonen et al., 1999; Mirabel
379 and Katz, 1974), under atmospheric conditions it may also play a negative role suppressing the
380 number concentrations of new particles by increasing aerosol surface area (Li et al. 2019).
381 Consistent with this, a negative relationship of the RH with NPF frequency was found for all the
382 sites of this study with very high R^2 for almost all of them ($R^2 > 0.80$). This is not simple to
383 interpret as solar radiation intensity, temperature, RH and CS are not independent variables, since

384 an increase in temperature of an air mass due to increased solar radiation will be associated with
385 reduced RH, which in turn affects the CS. The sites in Greece presented lower R^2 compared to the
386 other sites while, GRERU was found to have the weakest correlation ($R^2 = 0.22$). This may be due
387 to the different seasonality of the events found for the Greek sites (being more balanced within a
388 year), as there was increased frequency of NPF events for the seasons with higher RH compared to
389 other sites, making it a less important factor for their occurrence as found in the previous study by
390 Bousiotis et al., (2020). Growth rate on the other hand had a variable relationship, either positive or
391 negative, with only a handful of background sites having strong correlations. The German
392 background sites as well as FINRU, which were among the sites with the highest average RH
393 (average RH for GERRU is 81.9%, GERUB is 78.7% and FINUB is 80.1%) presented a negative
394 relationship between the RH and growth rate. DENRU (average RH at 75.7%) had a positive
395 relationship, which might indicate that the relationship between these two variables may vary
396 depending upon the RH range. Formation rate also appears to have a negative relationship with the
397 RH, though this relationship was significant ($R^2 > 0.40$) for only 6 sites, which once again in most
398 cases are sites with higher RH average conditions. Along with the results of the growth rate this
399 might indicate that the RH becomes a more important factor in the development of NPF events as
400 its values increase.

401

402 The normalised gradients once again provide some additional information. Regarding the NPF

403 frequency, it is found that the a_N^* was more negative at rural sites compared to roadside sites. This

404 indicates that the RH has a smaller effect at roadside sites, as other variables, such as the
405 atmospheric composition, are probably more important within the complex environment in this type
406 of site. Additionally, the relationship between a_N^* and average RH at the sites had a negative
407 relationship ($R^2 = 0.46$), which further shows that the RH becomes a more important factor at
408 higher values (Figure 4). Furthermore, at the sets of rural and roadside sites with R^2 higher than
409 0.40 for the relation between RH and the formation rate (UK and German sites), it was found that
410 the a_J^* was more negative at the rural sites which indicates that the RH is a more important factor at
411 rural sites compared to their respective roadside sites.

412

413 **3.1.3 Temperature**

414 Temperature can have both a direct and indirect effect in the development of NPF events, as it is
415 directly associated with the abundance of both biogenic and anthropogenic volatile carbon, which is
416 an important group of compounds whose oxidation products can participate in nucleation itself
417 (Lehtipalo et al., 2018; Rose et al., 2018), as well as in the growth of newly formed particles. It may
418 also have a negative effect on the particle size distributions or number concentrations through other
419 processes such as particle evaporation. Most of the sites of the present study presented a strong
420 relationship of NPF frequency with temperature, which in most cases was positive, though in many
421 cases (such as the Danish, Finnish and Spanish sites – figures S2b, d and e) there seems to be a peak
422 in the NPF frequency at some temperature, after which a decline starts (though being at the higher
423 end does not greatly affect the results). Sites with smaller R^2 (weaker association with temperature),

424 were mainly those that have a seasonal variation that favoured seasons other than summer. These
425 sites not only had weaker relationship of NPF frequency with temperature, but in most cases had a
426 negative relationship (background sites in Finland, Spain and Greece). The Finnish sites, having the
427 lowest average temperatures and a sufficient amount of data below zero temperature, show at all
428 three sites the possible presence of a peak in the NPF event frequency for temperatures below zero
429 (Figure S2d). This seems to be the cause of the weak relationships found there and they seem to be
430 associated with the formation rate J_{10} , which also seems to have an increasing trend below zero
431 degrees (Figure S2p). This may depend on the nucleation mechanism occurring, as cluster
432 evaporation rates of sulphuric acid clusters are sensitive to the ternary stabilising compound present
433 (Olenius et al., 2017), as well as the possible enhancement of growth mechanisms at lower
434 temperatures (below 5°C) by other chemical compounds in the atmosphere (i.e. nitric acid and
435 ammonia) as found by Wang et al., (2020). Laboratory experiments show that the characteristics of
436 organic aerosol forming from alpha-pinene is governed by gas phase oxidation (e.g. Ye et al. 2019).
437 In the real atmosphere, the higher temperature enhances the amount of biogenic vapours (e.g.
438 Paasonen et al. 2013) and, although the oxidation can be more efficient at higher temperatures, the
439 lower temperatures favour formation of more non-volatile compounds (Quéléver et al., 2019;
440 Stolzenburg et al. 2018; Ye et al. 2019).

441

442 Growth rate had a more uniform trend, with almost all sites having a positive relationship with
443 temperature (apart from GERRO, though with $R^2 = 0.00$). This relationship was very strong for

444 most sites ($R^2 > 0.60$ for 10 sites), which is also confirming the summer peak found for the growth
445 rate at most of these sites in other studies (Bousiotis et al., 2020; 2019). A rather strong relationship
446 ($R^2 > 0.50$) with temperature was also found for the formation rate for most sites, and was positive
447 for almost all sites (apart from FINRO with $R^2 = 0.01$ and the Greek sites with $R^2 < 0.47$). As with
448 the NPF frequency, in general the sites with a seasonal variation of events that favoured summer
449 had the strongest relationship (high R^2) of the temperature with formation rate, which might
450 indicate that this variable, either through its direct or indirect effect is an important one for the
451 seasonal variability of NPF events in a given area.

452

453 The normalised gradients for this variable did not present a clear trend among the areas studied,
454 other than presenting greater a_N^* for the sites with a summer peak in their NPF event seasonal
455 variation. As with other meteorological variables, the importance of this variable became smaller
456 with increased values in the average conditions for both the NPF frequency (Figure 5) and J_{10} ,
457 though these relationships were not significant (biased by the very low average temperatures and
458 different behaviour of the variables at the Finnish sites, without which the relationship becomes a
459 lot clearer as indicated in Figure S13). The variation though within the sites of the same area
460 (different sites in same country / region) appears to directly follow the variability of temperature,
461 showing that the temperature directly affects the occurrence of NPF events when other
462 meteorological factors remain constant, having a negative trend for all countries but Finland. The
463 a_J^* though is found to be greater (positively or negatively) at the rural background sites than at the

464 other two types of sites at all areas studied, showing that it is a more important factor for the
465 formation rate at this type of site compared to others (Figure 6).

466

467 **3.1.4 Wind speed**

468 Wind speed may have both a positive and a negative effect on the occurrence of NPF events. On
469 one hand, it may promote NPF events by the increased mixing of the condensable compounds in the
470 atmosphere as well as by reducing the CS. On the other hand, high wind speeds may suppress NPF
471 events due to increased dilution. It should be considered that the variability found is also affected by
472 the specific conditions found at each site. The wind speed measurements in many cases, especially
473 in urban sites, can be biased by the local topography or specific conditions found at each site, thus
474 representing the local conditions for this variable rather than the regional ones. Similarly,
475 measurements of wind speed at well sited meteorological stations may be more representative of
476 regional conditions, than of those affecting the sites of nucleation measurement. The sites in this
477 study presented mixed results, both in the importance as well as the effect of the wind speed
478 variability. Three different behaviours were found in the variation of NPF event frequency and wind
479 speed which appear to be associated with local conditions as they are almost uniformly found
480 among the sites within close proximity. Some sites presented a steady increase of NPF event
481 frequency with wind speed (Danish sites, UKUB, FINRU, SPAUB and GRERU), while others were
482 found to steadily decline with increasing wind speeds (German sites – it should be noted that the
483 German sites are the only ones that are located at a great distance from the sea), while some were

484 found to reach a peak and then decline, which also leads to smaller R^2 (UKRU, UKRO, SPARU and
485 to a lesser extent GREUB – figures S4a, e and f). The reasons for these differences between the
486 sites are very hard to distinguish as apart from the wind speed the origin and the characteristics of
487 these air masses play a crucial role. Following this, it appears that NPF frequency is very low or
488 zero for wind speeds close to calm for the sites with an increasing trend (as well as those that have a
489 peak and decline after), while the opposite is observed for the German sites where the maximum
490 NPF frequency is found for very low wind speeds (fig. S4c).

491

492 Similarly, the effect of different wind speeds upon the growth rate also varied a lot, though it was
493 found to be negative in all the cases where R^2 was higher than 0.50 (UKUB, DENRU, DENRO,
494 GERRU, GERUB and GREUB). Finally, the formation rate was found to have a significant
495 correlation ($R^2 > 0.40$) only at two sites (UKRO and DENRU), probably indicating that the
496 variability of the wind speed either does not affect this variable or its effect is rather small.

497

498 The normalised gradients did not have any notable relationship to either the NPF frequency or the
499 formation rate further confirming that the effect of the different wind speeds is not due to its
500 variability only, but it is also influenced by the characteristics of the incoming air masses as well as
501 specific local conditions found at each site.

502

503

504 3.1.5 Pressure

505 In almost all the sites with available data (apart from the Spanish), the NPF frequency presented a
506 positive relationship with high significance at all types of sites. The greater significance found at the
507 rural sites (apart from SPARU) indicates the increased importance of meteorological conditions in
508 the occurrence of NPF events at this type of site. The growth rate also presented a similar picture,
509 with positive relationships at all the background sites of this study except the ones in Greece ($R^2 >$
510 0.71) and FINUB (though with low R^2 at 0.02). This is probably associated with the seasonal
511 variation found in Greece where higher growth rates were found in summer, a period when
512 increased wind speeds and lower atmospheric pressure was found due to the Etesians, a pressure
513 system that develops in the region every summer (Kalkavouras et al., 2017). An interesting finding
514 is the negative gradients found at all the roadside sites, though the significance of these results is
515 relatively low ($R^2 < 0.43$) and always lower compared to the rural sites. The effects of pressure
516 above are not likely to be important. Once again however, this is not an independent variable and
517 higher pressure in summer tends to be associated with higher insolation and temperatures and lower
518 RH. Since most events occur in the warmer months of the year, this is probably the explanation for
519 the apparent effects of pressure. The formation rate presented relationships of low significance (R^2
520 < 0.47) for the sites of this study. Due to this, pressure should not be an important factor for the
521 formation rate at any type of site.

522

523 The normalised gradients did not present any clear trends, even for the NPF frequency for which the
524 results presented significant relationships at almost all sites.

525

526 **3.2 Atmospheric Composition**

527 The gradients, R^2 and p-values from the analysis of a number of air pollutants (SO_2 , NO_x , O_3 ,
528 organic compounds, sulphate and ammonia) and the CS, as well as the average conditions of these
529 variables are found in Table 4. The results for each site and variable are found in Figures S6 – S12.

530

531 **3.2.1 Sulphur dioxide (SO_2)**

532 Sulphur dioxide, as a precursor of H_2SO_4 , is considered as one of the main components associated
533 with the NPF process. According to nucleation theories and observations, H_2SO_4 is the most
534 important compound from which the initial clusters are formed, as well as one of the candidate
535 compounds for the initial steps of particle growth (Kirkby et al., 2011; Nieminen et al., 2010; Sipila
536 et al., 2010; Stolzenburg et al., 2020). As H_2SO_4 in the atmosphere is produced from oxidation
537 reactions of SO_2 it would be expected that increased concentrations of the latter would be associated
538 with increased values for all the variables associated with the NPF process. Contrary to this though,
539 the relationship of SO_2 concentrations with NPF frequency was found to be negative at all the sites
540 in this study with available data. This is expected as the average concentrations of SO_2 on NPF
541 event days was found to be lower compared to the average conditions in most cases as found by
542 Bousiotis et al., (2019; 2020). This relationship was relatively strong ($R^2 > 0.50$) in most areas with

543 an increased significance at roadside sites compared to their respective rural sites. As this is a
544 negative relationship, this may indicate that SO₂ is in sufficient concentrations for H₂SO₄ formation,
545 thus not suppressing the occurrence of NPF events, as well as showing that in increased
546 concentrations, it is a more important factor (or surrogate for a factor) in preventing the occurrence
547 of NPF events within the urban environment, as higher SO₂ is likely associated with increased co-
548 emitted particle pollution and hence CS. The growth rate on the other hand, presented mixed results
549 and the significance of the relationships is low in most cases, which makes these results unreliable.
550 Finally, the relationship of SO₂ concentrations with the formation rate was found to be positive at
551 all sites but SPARU and FINRU (which had the lowest concentrations across the sites with
552 available data). The significance of this relationship was rather low ($R^2 < 0.40$) for all but the
553 roadside sites. This suggests that higher H₂SO₄ concentrations favour greater formation rates (i.e.
554 more particles can be formed), rather than necessarily promoting nucleation itself because of the
555 competing effect of condensation onto the pre-existing particle population.

556

557 The normalised gradients a_N^* were found to be more negative at the background sites compared to
558 their respective roadside sites, as well as being less negative in the UK (where SO₂ is in greater
559 abundance) compared to the other sites with relatively significant relationships. Plotting the average
560 SO₂ concentrations with the normalised gradients a_N^* for the all sites (though not all had significant
561 relationships), a positive relationship with relatively high R^2 (when the extreme values from
562 Marylebone Road-UKRO are removed) is found which might indicate that while increased

563 concentrations are a negative factor in NPF event occurrence at a given site, in general the sites with
564 higher SO₂ concentrations on average present higher frequency for NPF events (Figures 7a and b).
565 This appears to be in agreement with Dall'Osto et al. (2018) who discussed the variable role of SO₂
566 depending on its concentrations. Similar findings for the effect of SO₂ were also found in previous
567 studies (Jung et al., 2006; 2008), relating particle acidity to NPF. Finally, no significant
568 relationships were found for the values of a_j^* as in most cases these relationships were rather weak.

569

570 **3.2.2 Nitrogen oxides or nitrogen dioxide (NO_x or NO₂)**

571 NO_x and NO₂ are directly associated with pollution, which can be a limiting factor for NPF events
572 as it increases the CS and may suppress the events (An et al., 2015), though with the reduction of
573 SO₂ concentrations achieved the last couple of decades, there is a possibility for oxidation products
574 of NO_x to become an important component for NPF (Wang et al., 2020). For almost all sites (apart
575 from GRERU) with available data a negative relationship between the NPF frequency and NO_x
576 concentrations (or NO₂ depending on the available data) was found. Similarly, for all the sites but
577 SPARU and GRERU, the correlations were relatively strong with $R^2 > 0.43$. The rural background
578 sites had a weaker relationship between the two variables compared to the urban sites, which is
579 probably associated with them having rather low concentrations and variability of NO_x (or NO₂),
580 making the variations of this factor less important. Growth rate had weaker correlations with NO_x
581 and different trends between the sites, either being positive or negative. The variable effect of NO_x
582 on particle growth, shifting HOMs volatility, was previously discussed by Yan et al. (2020). While

583 variability was found for the background sites, all roadside sites regardless of the strength of the
584 relationship had a positive relationship between NO_x and the growth rate. This may indicate the
585 different components associated with the growth process at each type of site which, as found in
586 other studies, can be related to compounds associated with combustion processes that take place
587 within the urban environment (Guo et al., 2020; Wang et al., 2017a). The formation rate presents
588 few cases of strong relationships, with variable trends (positive and negative). While much effort
589 was made to isolate the effect of NPF events by taking a shorter time frame before the event, the
590 effect of local pollution is still included, especially at the urban sites (which probably explains the
591 positive effect found).

592

593 The normalised gradients do not provide a significant result for the relationship of this variable with
594 either the frequency of the events or the formation rate. The only noteworthy points are the more
595 negative a_N^* at the rural background sites compared to the roadside sites in all the areas studied,
596 which shows the increased importance of a clean environment for NPF events to occur in areas
597 where condensable compounds are in lesser abundance, such as a rural environment. Additionally,
598 the negative gradients found at all the roadside sites, which increases the confidence that the events
599 extracted at the roadside sites are not pollution incidents but NPF events. However, it appears that
600 traffic pollution favours higher particle growth rates, although the components responsible for this
601 effect are unknown.

602

603 3.2.3 Ozone (O₃)

604 Ozone is typically the result of atmospheric photochemistry and is itself a source of hydroxyl
605 radical through photolysis, or ozonolysis of alkenes both during daytime and night-time (Fenske et
606 al., 2000). It might therefore be expected to act as an indicator of photochemical activity which
607 promotes the oxidation of SO₂ and VOCs. Ozone concentrations may be directly related to the
608 solar radiation intensity as well as the pollution levels in the area studied, and O₃ is considered as a
609 positive factor in the occurrence of NPF events (Woo et al., 2001; Berndt et al., 2006). As with the
610 solar radiation intensity, there is a strong relationship between O₃ concentration and the frequency
611 for NPF events. This positive relationship, which is in agreement with the higher concentrations of
612 O₃ found on NPF event days compared to average conditions for all sites in Bousiotis et al., (2019;
613 2020), was found to be stronger for the sites in northern Europe ($R^2 > 0.51$), while it was not
614 significant ($R^2 < 0.38$) for the sites in southern Europe (Spanish sites and GRERU), possibly
615 indicating that O₃ is a less important factor at the southern sites. Specifically for the Spanish sites
616 which have the highest average concentrations of O₃ with some extreme values (Querol et al.,
617 2017), the relationship of O₃ concentrations with the NPF frequency presents a unique trend (Figure
618 S8d), having a clear peak then a steady decline at both sites (though at different O₃ concentrations),
619 which is also responsible for the low correlations found (this trend seems to also occur at SPARU
620 for the growth rate and to a lesser extent for the formation rate as well, though for different O₃
621 concentration ranges – figures S8i and n). The specific variability found at the Spanish sites was
622 also studied by Carnerero et al., (2019). For sites with a marked seasonal variation in ozone,

623 associations with NPF may be artefactual due to correlations with other variables such as
624 temperature, RH and solar radiation intensity.

625
626 Unlike the solar radiation intensity though, the growth rate presents a negative relationship at the
627 sites where the relationship between these two variables was significant (UKRU, UKUB, DENUB
628 and FINRU), which might either be an indication of a polluted background that may have a
629 negative effect in the growth of the newly formed particles (though the trends found for NO_x
630 indicate differently) or specific chemical processes which cannot be identified due to the lack of
631 detailed chemical composition data. A significant relationship between O_3 and the formation rate
632 was only found for two sites (UKRO and DENRO, though the trends become a lot clearer if some
633 values are removed from the extreme lower or higher end). This way the relationships become
634 strong, but positive, for some areas and negative for some others without any clear trend (type or
635 location of the site, O_3 concentrations etc.). No clear relationship between these two variables was
636 found as the sites with strong relationship have both positive (DENRO) and negative (UKRO)
637 relationships and as a result no confident conclusions can be drawn.

638
639 As the correlations found were strong the normalised gradients for NPF frequency, when plotted
640 against the average concentrations of O_3 , present a negative correlation with relatively high R^2
641 (0.64), indicating that the O_3 is a more important factor in the occurrence of NPF events when in
642 lower concentrations (Figure 8). Finally, though with a low level of confidence for the southern

643 sites, the a_N^* were smaller at the southern sites compared to those in the north, up to one order of
644 magnitude between FINRU (furthest north rural background) and GRERU (furthest south rural
645 background).

646

647 **3.2.4 Organic compounds**

648 **3.2.4.1 Particulate organic carbon (OC)**

649 Organic carbon (OC) compounds in the secondary aerosol typically enter the particles via
650 condensational processes, with a role that becomes increasingly important as the size of the
651 particles becomes larger (Nieminen et al., 2010; Zhang et al., 2012; Shrivastava et al., 2017).
652 Particulate OC, the data for which is available in the present study, can be associated with pollution,
653 especially in the urban environment. Only a few of the sites of the present study were found to have
654 a relatively strong negative relationship ($R^2 > 0.50$) of particulate OC with the NPF frequency
655 (UKUB, UKRO and DENRU). Regardless though of the strength of this relationship, all other sites
656 (apart from FINRU) had a negative relationship between these two variables as well, consistent
657 with increased concentrations of particulate OC being associated with increased pollution, which
658 elevate the CS, suppressing the occurrence of NPF events. Growth rate on the other hand was found
659 to have a positive relationship ($R^2 > 0.40$) for most of the sites. This relationship appeared to be
660 stronger (higher R^2) at the roadside sites with available data compared to their respective rural
661 background sites. The relationship between particulate OC and the growth rate was positive at all
662 the sites with available data regardless of their significance showing that, despite its effect in the

663 occurrence of NPF events, it is still a favourable variable for the growth of the particles. The
664 formation rate was found to have a significant relationship with particulate OC concentrations at
665 half of the sites with available data (UKUB, UKRO, DENRU, DENRO).

666

667 The normalised gradients for this variable did not present any noteworthy relationships with either
668 the type of site or the concentrations of OC at a given site.

669

670 **3.2.4.2 Volatile organic compounds (VOCs)**

671 Many volatile organic compounds have been found to be associated with the NPF process. Benzene,
672 toluene, ethylbenzene, m-p-xylene, o-xylene and trimethylbenzenes have been reported to be able to
673 form Highly Oxygenated Organic Molecules (HOMs) in flow tubes (Wang et al., 2017a; Molteni et
674 al., 2018), which may act as contributors to particle nucleation and/or growth. Xylenes, and to a
675 lesser extent trimethylbenzenes, are the most efficient at forming HOMs. Benzene and toluene are
676 less efficient and will form more volatile HOMs. These HOMs may all be too volatile to form new
677 particles, though this is not yet confirmed. Chamber studies involving H₂SO₄ and trimethylbenzene
678 oxidation products were associated with high formation rates when measuring J_{1.5} (Metzger et al.,
679 2010). All these HOMs though will be sufficiently involatile to contribute to particle growth. Those
680 with higher oxygen content or carbon number will be classed as LVOC and if they dimerise, they
681 will form ELVOC (Bianchi et al., 2019). Monoterpenes can also form HOMs which drive both the
682 formation (Ehn et al., 2014; Riccobono et al., 2014) and growth (Tröstl et al., 2016), while isoprene

683 can act as a sink for hydroxyl radical (Kiendler-Scharr et al., 2009) and is not as effective in HOM
684 and secondary organic aerosol formation compared to monoterpenes (McFiggans et al., 2019).
685
686 Volatile organic compound data were available for three of the sites of this study (Table S2). Two
687 of the sites with VOC data were from the rural background and the roadside site in the UK. Most of
688 the compounds are associated with combustion sources and were found to have a negative
689 relationship with NPF event occurrence at both sites, with high R^2 ($R^2 > 0.50$) in most cases.
690 Additionally, isoprene, which may have either biogenic or anthropogenic sources (Wagner and
691 Kuttler, 2014) was also found to have a negative relationship with NPF event occurrence at
692 Marylebone Road-UKRO, though with low R^2 (0.07). This result is in line with the VOCs being
693 strongly correlated with particulate OC (which presented a negative relationship with NPF event
694 frequency, as discussed in Section 3.2.4.1), as well as with the CS (which also presented a negative
695 relationship with NPF event frequency, as mentioned in Section 3.2.6), further associating these
696 compounds with combustion emissions.
697
698 Growth rate was found to have a positive relationship with VOCs in almost all cases for both UK
699 sites. Few exceptions were found (with only 1,3 butadiene having a relatively high R^2) which
700 presented a negative relationship with the growth rate in rural Harwell-UKRU. Finally, the
701 formation rate presented a different behaviour between the two sites. At UKRU, the relationship
702 was unclear in most cases, with a group of VOCs presenting a negative relationship with the

703 formation rate (ethane, ethene, propane, 1,3 butadiene, toluene, ethylbenzene, o-xylene and 1,2,4
704 trimethylbenzene – with $R^2 > 0.40$), two VOCs presented a rather clear positive relationship with
705 the formation rate (iso-pentane and 2-methylbenzene) and the rest of the VOCs had an unclear
706 relationship. At UKRO though, VOCs presented a positive relationship with the formation rate (for
707 particles of diameter 16 nm). This is probably due to the fact that these VOCs are associated with
708 pollution emissions (as mentioned earlier) and though a smaller time window was chosen to avoid
709 including the effect of the morning rush hour traffic, this is very difficult in the traffic polluted
710 environment of Marylebone Road.

711

712 As Hyytiälä (FINRU) is a rural background site far from the direct effect of combustion emissions,
713 different VOCs were measured, which mainly originate from biogenic sources rather than
714 anthropogenic ones. The results were mixed and less clear compared to those from the UK sites
715 (mainly due to the smaller dataset), and three groups were found depending on their relationship
716 with NPF frequency. The first group, including acetonitrile, acetic acid and methyl ethyl ketone
717 (MEK) presented a slight positive relationship. The second group presented a negative relationship,
718 with the VOCs in this group being monoterpenes, methacroleine, benzene, isoprene and toluene
719 (only the last two have $R^2 > 0.50$). Finally, the third group included VOCs that presented a peak and
720 then a decline for higher concentrations including methanol, and acetone. Two groups of VOCs
721 were found depending on their relationship with the growth rate. The ones with a positive
722 relationship being methanol, acetonitrile, acetone, acetic acid, isoprene, methacroleine,

723 monoterpenes and toluene, while acetaldehyde, MEK and benzene had a negative relationship, with
724 relatively high R^2 in most cases. Finally, the results with the formation rate were unclear with only a
725 handful presenting weak ($R^2 < 0.21$) positive (methanol, acetic acid and benzene) or negative
726 (MEK) relationships that do not appear to be significant. The normalised gradients cannot be used
727 for VOCs as there are very few sites with available data.

728

729 **3.2.5 Sulphate (SO_4^{2-})**

730 Sulphate (SO_4^{2-}) is a major secondary constituent of aerosols. Secondary SO_4^{2-} aerosols largely arise
731 from either gas phase reaction between SO_2 and OH, or in the aqueous phase by the reaction of SO_2
732 and O_3 or H_2O_2 , or NO_2 (Hidy et al., 1994). In environments where SO_4^{2-} chemistry is dominant
733 (i.e. remote areas), SO_4^{2-} and ammonium (bi) sulphate ($(\text{NH}_4)_2\text{SO}_4$ and NH_4HSO_4) particles are a
734 large relative contributor to aerosol mass, while this contribution is lower in environments where
735 other emissions are also significant (i.e. urban areas where the secondary NO_3^- relative contribution
736 is a lot higher). While not well established, a possible relationship of SO_4^{2-} -containing compounds
737 and variables of NPF events was found in previous studies (Beddows et al., 2015; Minguillón et al.,
738 2015; Wang et al., 2017b). In the present study, only a few sites had SO_4^{2-} data available, for PM_1
739 (FINRU), $\text{PM}_{2.5}$ (Danish sites) or PM_{10} (rest of the sites). While this data cannot be considered as
740 directly associated with the ultrafine particles, for two sites with available ACSM data for ultrafine
741 particles, the direct comparison between SO_4^{2-} aerosol in PM and in the range of particles of about
742 50 nm, very high correlations were found (results not included). For all the sites with available data

743 the NPF frequency presented a negative relationship. The significance of this relationship was
744 found to be relatively high ($R^2 > 0.50$) only for background sites (apart from GERRU, which has
745 rather low concentrations and probably different mechanisms for the NPF events). Similarly, the
746 growth rate presented a significant relationship ($R^2 > 0.40$) for the same background sites (apart
747 from FINRU), though this relationship was found to be positive at all sites regardless of its
748 significance. Finally, the formation rate did not present a clear trend as it was found to have both
749 negative and positive relationships for different sites. This relationship was significant only for two
750 rural sites (UKRU and DENRU) and as a result no conclusions can be reached.

751

752 The normalised gradients cannot be used for any analysis on sulphate as the measurements available
753 are from different particle size ranges.

754

755 **3.2.6 Gaseous ammonia (NH_3)**

756 Ammonia (NH_3) can be an important compound in the nucleation process according to the ternary
757 theory (Kirkby et al., 2011; Napari et al., 2002). It was found that elevations in NH_3 concentrations
758 can lead to elevations to NPF rate (Lehtipalo et al., 2018) and it was also found to be an important
759 factor for NPF event occurrence even when stronger bases are present in high concentrations
760 (Glasoe et al., 2015). No significant variation was found though between event and non-event days
761 in a previous study in Harwell - UKRU (Bousiotis et al., 2019). Data for gaseous ammonia was only
762 available for UKRU and presented a positive relationship with NPF frequency, until reaching a

763 peak point. Further increase in NH_3 concentrations presented a decline with NPF frequency (Figure
764 S11a), which might be due to its association with increased pollution levels. It presented a clear
765 positive relationship with both the growth rate (though it also appears to decline at high
766 concentrations) and the formation rate, consistent with its well-established role in accelerating both
767 of these processes (Kirkby et al. 2011; Stolzenburg et al., 2020).

768

769 **3.2.7 Condensation sink (CS)**

770 The CS is a measure of the rate at which molecules will condense onto pre-existing aerosols
771 (Lehtinen et al., 2003). It is highly dependent on the number and size of the particles in the
772 atmosphere and as a result it is expected to be affected by both the local emissions within the urban
773 environment as well as the formation and growth of the particles due to NPF events. As a result, for
774 the specific metric a time frame before the events are in full development was chosen (05:00 to
775 10:00 LT) to avoid including the effect of the NPF events and provide a picture of the atmospheric
776 conditions that preceded the NPF events. With this data, the NPF frequency presented very strong
777 relationships with the condensation sink. Two groups of sites were found though; those which had a
778 positive relationship and those with a negative relationship. In the first group are the sites in
779 Germany and Greece while all others had a negative relationship. This grouping follows the trend
780 between the countries, the sites of which presented a greater or smaller CS on NPF event days
781 according to the findings in Bousiotis et al., (2019; 2020) (having positive or negative gradients
782 respectively), though it is unknown what causes this behaviour (at the German sites and GREUB it

783 may be associated with the very high formation rates on NPF event days). While the gradients from
784 this analysis cannot be used for direct comparisons, a trend was found for which the gradients were
785 more positive or negative at the rural sites compared to their respective roadside sites, which might
786 indicate the greater importance of the variability of the CS at the rural sites in the occurrence of
787 NPF events.

788

789 The growth rate was positively correlated with the CS for most of the sites, with relatively strong
790 relationships ($R^2 > 0.40$) for about half of them. As the CS is a metric of pre-existing particles, it is
791 also associated with the level of pollution in a given area. The increased significance and gradient
792 found at the rural sites probably indicates the importance of enhanced presence of condensable
793 compounds in a cleaner environment, which in many cases are associated with the moderate
794 presence of pollution. The formation rate was also found to have a positive relationship with the CS.
795 This relationship was more significant at the roadside sites of this study, a result which to some
796 extent is biased by the presence of increased traffic emissions found in the timeframe chosen. While
797 to an extent, increased presence of condensable compounds can be favourable for greater formation
798 rates, this result should be considered with great caution.

799

800 The normalised gradients a_N^* followed a similar trend as those found with the initial analysis. These
801 gradients were found to be more positive or negative, depending on the trend of the given area, at
802 the rural sites compared to their roadside sites. The urban background sites did not always have a

803 uniform behaviour (though in UK, Denmark and Finland these were between the rural site and the
804 roadside site), due to their more diverse character compared to the other two types of sites.

805

806 **3.3 Association of the Effect of the Variables**

807 The Pearson correlation coefficients for the variables studied on each site are found in Table S1.

808 The relatively strong relationship between the solar radiation intensity, temperature and O₃ found,
809 as well as their anticorrelation with the RH may lead to the conclusion that not all these factors play
810 a role in NPF events, but their visible effect is the result of their relationship with each other. There
811 is a similar case with the association of the CS and NO_x (or NO₂), and OC, as well as SO₂,
812 especially at urban sites. However, the factors affect different outcomes differently, as for example
813 the solar radiation intensity does not seem to be as important a factor for the growth rate as
814 temperature, or O₃ does not seem to be strongly associated with either the formation or the growth
815 rate. This is further established by the fact that some of these variables do not correlate well at the
816 southern sites, but still appear to be associated with either the frequency of NPF events or the
817 growth or nucleation rate. The effects of all of these factors have been demonstrated in both
818 laboratory and atmospheric studies in the past and were discussed earlier in this paper. By the
819 analysis provided in the present study, the effect of each of these variables is further established,
820 providing an association of each one of these variables with either the formation or the growth
821 mechanism. However, RH does not seem to be a consistent factor in any mechanism, and it appears

822 that its effect is dependent on location specific conditions, although it was the variable with the
823 most consistent relation with NPF event frequency at almost all sites.

824

825 **3.4 Relationship to a previous multi-station European study**

826 The findings of our study in respect of the background sites show many similarities with the
827 conclusions drawn in the previous multi-station study in Europe by Dall'Osto et al. (2018) despite
828 the two studies using several different sampling stations as well as some in common. Both studies
829 point towards the influence of variables such as solar radiation intensity and CS upon the
830 occurrence of NPF events. The previous study suggested that different compounds participate in the
831 growth of the particles, depending on the area considered. Thus, for northern and southern sites the
832 growth of the particles is suggested to be driven mainly by organic compounds, while for the sites
833 in central Europe sulphate plays a more important role. These findings are confirmed by the present
834 study, as the growth rate was found to correlate better with organic compounds for the rural sites in
835 Finland and Greece, while SO_4^{2-} presented a stronger relationship with the growth rate for the
836 Danish and German sites (the latter presented high gradient values but low R^2 due to a decline at
837 higher SO_4^{2-} concentrations – figure S10i, probably associated with NPF events being suppressed
838 by increased pollution). The growth of the particles at the rural background site in the UK,
839 characterised as “Overlap” in the previous study, was found to be strongly associated with both
840 organic compounds and sulphate, consistent with it being in the central group.

841

842 The seasonality of NPF events at northern sites was hard to explain in the previous study, and the
843 possible effect of low temperature was considered. In the present study, the Finnish background
844 sites presented a double-peak relationship of NPF frequency with temperature, with one of the
845 peaks being below zero degrees. This might point to the possibility of different compounds driving
846 the events for different temperature ranges, as well as the increased nucleation rate of H₂SO₄ at
847 lower temperatures (Kirkby et al., 2011; Yan et al., 2018), which makes the occurrence of NPF
848 events more probable at lower temperatures in a region with low SO₂ concentrations.

849

850 4. CONCLUSIONS

851 The present study attempts to explain the effect of several meteorological and atmospheric variables
852 on the occurrence and development of NPF events, by using a large-scale dataset. More than 85
853 site-years of data from 16 sites from six countries in Europe were analysed for NPF events. A total
854 of 1952 NPF events with consequent growth of the newly formed particles were extracted and with
855 the use of binned linear regression, the relationship between three variables associated with NPF
856 events (NPF event frequency, formation and growth rate) with meteorological conditions and
857 atmospheric composition was studied. Among the meteorological conditions, solar radiation
858 intensity, temperature and atmospheric pressure presented a positive relationship with the
859 occurrence of NPF events in the majority of the sites (though exceptions were found as well, mostly
860 in the southern sites), either promoting the formation or growth rate. RH presented a negative
861 relationship with NPF event frequency which in most cases was associated with it being a limiting

862 factor on particle formation at higher average values. Wind speed on the other hand presented
863 variable results, appearing to depend on the location of the sites rather than their type. This shows
864 that while wind speed can be a factor in NPF event occurrence, the origin of the incoming air
865 masses also plays a very important role. In most cases, meteorological conditions, such as
866 temperature or RH appeared to be more important factors in NPF event occurrence at rural sites
867 compared to urban sites, suggesting that NPF events are driven more by them at this type of site
868 compared to urban environments and the more complex chemical interactions found there.
869 Additionally, while some meteorological variables appeared to play a crucial role in the occurrence
870 of NPF events, this role appears to become less important at higher values when a positive relation
871 was found (or lower when a negative relation was found).

872

873 The results for the levels of atmospheric pollutants presented a more interesting picture as most of
874 these, which appear to be either directly or indirectly associated with the NPF process were found to
875 have negative relationships with NPF frequency. This is probably due to the fact that increased
876 concentrations of such compounds are associated with more polluted conditions, which are a
877 limiting factor in the occurrence of NPF events, as was found with the negative relationship
878 between the CS and NPF frequency in most cases. Thus, SO₂, NO_x (or NO₂), particulate OC and
879 SO₄²⁻ concentrations were negatively correlated with NPF frequency in most cases. Average SO₂
880 concentrations appeared to correlate positively with the normalised NPF event frequency gradients
881 with a relatively significant correlation, indicating that while increasing concentrations have a

882 negative impact in the occurrence of NPF events at a given site, in general sites with higher SO₂
883 concentrations have higher frequency for NPF events. Conversely, these compounds in many cases
884 had a positive relationship (not always though with high significance) with the other variables
885 considered. Thus, particulate OC (and VOCs where data was available) and SO₄²⁻ consistently had a
886 positive relationship with the growth rate, while SO₂ was positively associated with both the
887 formation and growth rate in most cases. Finally, O₃ was positively correlated with NPF event
888 frequency at all sites in this study, though it presented variable results with the other two variables.
889 As with some meteorological conditions it was found that at sites with increased concentrations of
890 O₃, its importance as a factor was decreased, which to some extent can be related with the high CS
891 associated with peak summer O₃ days in southern Europe.

892

893 It should be noted that the variables considered are in many cases inter-related (e.g. temperature and
894 RH) and this considerably complicates the interpretation in terms of causal factors. Large datasets
895 are very useful in providing more uniform results by removing the possible bias of short period
896 extremities, which may lead to wrong assumptions. This study, apart from providing insights into
897 the effect of a number of variables on the occurrence and development of NPF events in
898 atmospheric conditions across Europe, also shows the differences that climatic, land use and
899 atmospheric composition variations cause to those effects. Such variations are probably the cause of
900 the differences found among previous studies. Following from this, the importance of a high-

901 resolution measurement network, both spatially and temporally is underlined, as it can help in
902 elucidating the mechanisms of new particle formation in the real atmosphere.

903

904 **DATA ACCESSIBILITY**

905 Data supporting this publication are openly available from the UBIRA eData repository at

906 <https://doi.org/10.25500/edata.bham.00000491>

907

908 **AUTHOR CONTRIBUTIONS**

909 The study was conceived and planned by RMH who also contributed to the final manuscript, and

910 DB who also carried out the analysis and prepared the first draft of the manuscript. AM, JKN, CN,

911 JVN, HP, NP, AA, GK, SV and KE have provided with the data for the analysis. JB provided help

912 with analysis of the data. FDP provided advice on the analysis. MDO, XQ and TP contributed to the

913 final manuscript.

914

915 **COMPETING INTERESTS**

916 The authors have no conflict of interests.

917

918 **ACKNOWLEDGMENTS**

919 This work was supported by the National Centre for Atmospheric Science funded by the U.K.

920 Natural Environment Research Council (R8/H12/83/011).

921 **REFERENCES**

922

923 Aalto, P., Hämeri, K., Becker, E. D. O., Weber, R., Salm, J., Mäkelä, J. M., Hoell, C., O'Dowd, C.
924 D., Karlsson, H., Hansson, H., Väkevä, M., Koponen, I. K., Buzorius, G. and Kulmala, M.: Physical
925 characterization of aerosol particles during nucleation events, *Tellus, Ser. B Chem. Phys. Meteorol.*,
926 53(4), 344–358, doi:10.3402/tellusb.v53i4.17127, 2001.

927

928 Alam, A., Shi, J. P. and Harrison, R. M.: Observations of new particle formation in urban air, *J.*
929 *Geophys. Res. Atmos.*, 108(D3), n/a-n/a, doi:10.1029/2001JD001417, 2003.

930

931 An, J., Wang, H., Shen, L., Zhu, B., Zou, J., Gao, J. and Kang, H.: Characteristics of new particle
932 formation events in Nanjing, China: Effect of water-soluble ions, *Atmos. Environ.*, 108, 32–40,
933 doi:10.1016/j.atmosenv.2015.01.038, 2015.

934

935 Bae, M.-S., Schwab, J. J., Hogrefe, O., Frank, B. P., Lala, G. G. and Demerjian, K. L.:
936 Characteristics of size distributions at urban and rural locations in New York, *Atmos. Chem. Phys.*
937 *Discuss.*, 10(1), 69–108, doi:10.5194/acpd-10-69-2010, 2010.

938

939 Beddows, D. C. S., Harrison, R. M., Green, D. C. and Fuller, G. W.: Receptor modelling of both
940 particle composition and size distribution from a background site in London, UK, *Atmos. Chem.*
941 *Phys.*, 15(17), 10107–10125, doi:10.5194/acp-15-10107-2015, 2015.

942

943 Beddows, D. C. S. and Harrison, R. M.: Receptor modelling of both particle composition and size
944 distribution from a background site in London , UK – a two-step approach', pp. 4863–4876, 2019.

945

946 Berland, K., Rose, C., Pey, J., Culot, A., Freney, E., Kalivitis, N., Kouvarakis, G., Cerro, J. C., Mallet,
947 M., Sartelet, K., Beckmann, M., Bourriane, T., Roberts, G., Marchand, N., Mihalopoulos, N. and
948 Sellegri, K.: Spatial extent of new particle formation events over the Mediterranean Basin from
949 multiple ground-based and airborne measurements, *Atmos. Chem. Phys.*, 17(15), 9567–9583,
950 doi:10.5194/acp-17-9567-2017, 2017.

951

952 Berndt, T., Böge, O. and Stratmann, F.: Formation of atmospheric H₂SO₄H₂O particles in the
953 absence of organics: A laboratory study, *Geophys. Res. Lett.*, 33(15), 2–6,
954 doi:10.1029/2006GL026660, 2006.

955

956 Bianchi, F., Kurtén, T., Riva, M., Mohr, C., Rissanen, M. P., Roldin, P., Berndt, T., Crouse, J. D.,
957 Wennberg, P. O., Mentel, T. F., Wildt, J., Junninen, H., Jokinen, T., Kulmala, M., Worsnop, D. R.,
958 Thornton, J. A., Donahue, N., Kjaergaard, H. G. and Ehn, M.: Highly oxygenated organic molecules
959 (HOM) from gas-phase autoxidation involving peroxy radicals: A key contributor to atmospheric
960 aerosol, *Chem. Rev.*, 119, 3472–3509, doi:10.1021/acs.chemrev.8b00395, 2019.

961 Bigi, A. and Harrison, R. M.: Analysis of the air pollution climate at a central urban background site,
962 *Atmos. Environ.*, 44(16), 2004–2012, doi:10.1016/j.atmosenv.2010.02.028, 2010.
963

964 Birmili, W., Weinhold, K., Rasch, F., Sonntag, A., Sun, J., Merkel, M., Wiedensohler, A., Bastian,
965 S., Schladitz, A., Löschau, G., Cyrus, J., Pitz, M., Gu, J., Kusch, T., Flentje, H., Quass, U., Kaminski,
966 H., Kuhlbusch, T. A. J., Meinhardt, F., Schwerin, A., Bath, O., Ries, L., Wirtz, K. and Fiebig, M.:
967 Long-term observations of tropospheric particle number size distributions and equivalent black
968 carbon mass concentrations in the German Ultrafine Aerosol Network (GUAN), *Earth Syst. Sci. Data*,
969 8(2), 355–382, doi:10.5194/essd-8-355-2016, 2016.
970

971 Bousiotis, D., Pope, F. D., Beddows, D. C., Dall’Osto, M., Massling, A., Nøjgaard, J. K.,
972 Nørdestrom, C., Niemi, J. V., Portin, H., Petäjä, T., Perez, N., Alastuey, A., Querol, X., Kouvarakis,
973 G., Vratolis, S., Eleftheriadis, K., Wiedensohler, A., Weinhold, K., Merkel, M., Tuch, T., and
974 Harrison, R. M.: An Analysis of New Particle Formation (NPF) at Thirteen European Sites, *Atmos.*
975 *Chem. Phys. Discuss.*, <https://doi.org/10.5194/acp-2020-414>, in review, 2020.
976

977 Bousiotis, D., Osto, M., Beddows, D. C. S., Pope, F. D. and Harrison, R. M.: Analysis of new
978 particle formation (NPF) events at nearby rural, urban background and urban roadside sites, *Atmos.*
979 *Chem. Phys.*, 19, 5679–5694, 2019.
980

981 Brines, M., Dall’Osto, M., Beddows, D. C. S., Harrison, R. M., Gómez-Moreno, F., Núñez, L.,
982 Artíñano, B., Costabile, F., Gobbi, G. P., Salimi, F., Morawska, L., Sioutas, C. and Querol, X.: Traffic
983 and nucleation events as main sources of ultrafine particles in high-insolation developed world cities,
984 *Atmos. Chem. Phys.*, 15(10), 5929–5945, doi:10.5194/acp-15-5929-2015, 2015.
985

986 Carnerero, C., Pérez, N., Petäjä, T., Laurila, T. M., Ahonen, L. R., Kontkanen, J., Ahn, K. H.,
987 Alastuey, A. and Querol, X.: Relating high ozone, ultrafine particles, and new particle formation
988 episodes using cluster analysis, *Atmos. Environ. X*, 4(October), doi:10.1016/j.aeaoa.2019.100051,
989 2019.
990

991 Charron, A. and Harrison, R. M.: Primary particle formation from vehicle emissions during exhaust
992 dilution in the roadside atmosphere, *Atmos. Environ.*, 37(29), 4109–4119, doi:10.1016/S1352-
993 2310(03)00510-7, 2003.
994

995 Charron, A., Birmili, W. and Harrison, R. M.: Fingerprinting particle origins according to their size
996 distribution at a UK rural site, *J. Geophys. Res. Atmos.*, 113(7), 1–15, doi:10.1029/2007JD008562,
997 2008.
998

999 Charron, A., Degrendele, C., Laongsri, B. and Harrison, R. M.: Receptor modelling of secondary and
1000 carbonaceous particulate matter at a southern UK site, *Atmos. Chem. Phys.*, 13(4), 1879–1894,

1001 doi:10.5194/acp-13-1879-2013, 2013.
1002
1003 Cheung, H. C., Chou, C. C.-K., Huang, W.-R. and Tsai, C.-Y.: Characterization of ultrafine particle
1004 number concentration and new particle formation in an urban environment of Taipei, Taiwan, *Atmos.*
1005 *Chem. Phys.*, 13(17), 8935–8946, doi:10.5194/acp-13-8935-2013, 2013.
1006
1007 Chu, B., Kerminen, V., Bianchi, F., Yan, C., Petäjä, T. and Kulmala, M.: Atmospheric new particle
1008 formation in China, *Atmos. Chem. Phys.*, 19, 115–138, doi:10.5194/acp-2018-612, 2019
1009
1010 Dada, L., Paasonen, P., Nieminen, T., Buenrostro Mazon, S., Kontkanen, J., Peräkylä, O.,
1011 Lehtipalo, K., Hussein, T., Petäjä, T., Kerminen, V. M., Bäck, J. and Kulmala, M.: Long-term
1012 analysis of clear-sky new particle formation events and nonevents in Hyytiälä, *Atmos. Chem. Phys.*,
1013 17(10), 6227–6241, doi:10.5194/acp-17-6227-2017, 2017.
1014
1015 Dai, L., Wang, H., Zhou, L., An, J., Tang, L., Lu, C., Yan, W., Liu, R., Kong, S., Chen, M., Lee, S.
1016 and Yu, H.: Regional and local new particle formation events observed in the Yangtze River Delta
1017 region, China, *J. Geophys. Res.*, 122(4), 2389–2402, doi:10.1002/2016JD026030, 2017.
1018
1019 Dal Maso, M., Kulmala, M., Riipinen, I., Wagner, R., Hussein, T., Aalto, P. P. and Lehtinen, K. E.
1020 J.: Formation and growth of fresh atmospheric aerosols: Eight years of aerosol size distribution data
1021 from SMEAR II, Hyytiälä, Finland, *Boreal Environ. Res.*, 10(5), 323–336,
1022 doi:10.1016/j.ijpharm.2012.03.044, 2005.
1023
1024 Dall’Osto, M., Beddows, D. C. S., Asmi, A., Poulain, L., Hao, L., Freney, E., Allan, J. D.,
1025 Canagaratna, M., Crippa, M., Bianchi, F., De Leeuw, G., Eriksson, A., Swietlicki, E., Hansson, H.
1026 C., Henzing, J. S., Granier, C., Zemannkova, K., Laj, P., Onasch, T., Prevot, A., Putaud, J. P., Sellegri,
1027 K., Vidal, M., Virtanen, A., Simo, R., Worsnop, D., O’Dowd, C., Kulmala, M. and Harrison, R. M.:
1028 Novel insights on new particle formation derived from a pan-european observing system, *Sci. Rep.*,
1029 8(1), 1–11, doi:10.1038/s41598-017-17343-9, 2018.
1030
1031 Dall’Osto, M., Querol, X., Alastuey, A., O’Dowd, C., Harrison, R. M., Wenger, J. and Gómez-
1032 Moreno, F. J.: On the spatial distribution and evolution of ultrafine particles in Barcelona, *Atmos.*
1033 *Chem. Phys.*, 13(2), 741–759, doi:10.5194/acp-13-741-2013, 2013.
1034
1035 Dall’Osto, M., Beddows, D. C. S., Pey, J., Rodriguez, S., Alastuey, A., M. Harrison, R. and Querol,
1036 X.: Urban aerosol size distributions over the Mediterranean city of Barcelona, NE Spain, *Atmos.*
1037 *Chem. Phys.*, 12(22), 10693–10707, doi:10.5194/acp-12-10693-2012, 2012.
1038
1039 Ehn, M., Thornton, J. A., Kleist, E., Sipilä, M., Junninen, H., Pullinen, I., Springer, M., Rubach, F.,
1040 Tillmann, R., Lee, B., Lopez-Hilfiker, F., Andres, S., Acir, I. H., Rissanen, M., Jokinen, T.,

1041 Schobesberger, S., Kangasluoma, J., Kontkanen, J., Nieminen, T., Kurtén, T., Nielsen, L. B.,
1042 Jørgensen, S., Kjaergaard, H. G., Canagaratna, M., Maso, M. D., Berndt, T., Petäjä, T., Wahner, A.,
1043 Kerminen, V. M., Kulmala, M., Worsnop, D. R., Wildt, J. and Mentel, T. F.: A large source of low-
1044 volatility secondary organic aerosol, *Nature*, 506(7489), 476–479, doi:10.1038/nature13032, 2014.
1045
1046 Fenske, J. D., Hasson, A.S., Paulson, S. E., Kuwata, K. T., Ho, A., Houk, K. N.: The Pressure
1047 Dependence of the OH Radical Yield from Ozone Alkene Reactions *J Phys Chem A*, 104 7821, 2000
1048
1049 Fuchs, N. A. and Sutugin, A. G.: Highly dispersed aerosols, *Top. Curr. Aerosol Res.*, 1,
1050 doi:https://doi.org/10.1016/B978-0-08-016674-2.50006-6, 1971.
1051
1052 Glasoe, W. a, Volz, K., Panta, B., Freshour, N., Bachman, R., Hanson, D. R., McMurry, P. H. and
1053 Jen, C.: Sulfuric acid nucleation: An experimental study of the effect of seven bases, , 1933–1950,
1054 doi:10.1002/2014JD022730, 2015.
1055
1056 Größ, J., Hamed, A., Sonntag, A., Spindler, G., Manninen, H. E., Nieminen, T., Kulmala, M.,
1057 Hörrak, U., Plass-Dülmer, C., Wiedensohler, A., and Birmili, W.: Atmospheric new particle
1058 formation at the research station Melpitz, Germany: connection with gaseous precursors and
1059 meteorological parameters, *Atmos. Chem. Phys.*, 18, 1835–1861, https://doi.org/10.5194/acp-18-
1060 1835-2018, 2018.
1061
1062 Guo, S., Hu, M., Peng, J., Wu, Z., Zamora, M. L., Shang, D., Du, Z., Zheng, J., Fang, X., Tang, R.,
1063 Wu, Y., Zeng, L., Shuai, S., Zhang, W., Wang, Y., Ji, Y., Li, Y., Zhang, A. L., Wang, W., Zhang, F.,
1064 Zhao, J., Gong, X., Wang, C., Molina, M. J. and Zhang, R.: Remarkable nucleation and growth of
1065 ultrafine particles from vehicular exhaust, *Proc. Nat. Acad. Sci. U. S. A.*, 117(7), 3427–3432,
1066 doi:10.1073/pnas.1916366117, 2020.
1067
1068 Hallar, A. G., Petersen, R., McCubbin, I. B., Lowenthal, D., Lee, S., Andrews, E. and Yu, F.:
1069 Climatology of new particle formation and corresponding precursors at storm peak laboratory,
1070 *Aerosol Air Qual. Res.*, 16(3), 816–826, doi:10.4209/aaqr.2015.05.0341, 2016.
1071
1072 Hamed, A., Korhonen, H., Sihto, S. L., Joutsensaari, J., Jrvinen, H., Petäjä, T., Arnold, F.,
1073 Nieminen, T., Kulmala, M., Smith, J. N., Lehtinen, K. E. J. and Laaksonen, A.: The role of relative
1074 humidity in continental new particle formation, *J. Geophys. Res. Atmos.*, 116(3), 1–12,
1075 doi:10.1029/2010JD014186, 2011.
1076
1077 Harrison, R. M.: Urban atmospheric chemistry: A very special case for study, *npj Clim. Atmos. Sci.*,
1078 1(1), 5, doi:10.1038/s41612-017-0010-8, 2017.
1079

1080 Henschel, H., Kurtén, T., Vehkamäki, H.: Computational study on the effect of hydration on new
1081 particle formation in the sulfuric acid/ammonia and sulfuric acid/dimethylamine systems, *J. Phys.*
1082 *Chem. A* 2016, 120, 11, 1886–1896, 2016.
1083
1084 Hidy, G. M.: Atmospheric sulfur and nitrogen oxides, Academic Press, ISBN: 9781483288666,
1085 1994
1086
1087 Hietikko, R., Kuuluvainen, H., Harrison, R. M., Portin, H., Timonen, H., Niemi, J. V and Rönkkö,
1088 T.: Diurnal variation of nanocluster aerosol concentrations and emission factors in a street canyon,
1089 *Atmos. Environ.*, 189, 98–106, doi:10.1016/j.atmosenv.2018.06.031, 2018.
1090
1091 Iida, K., Stolzenburg, M. R., McMurry, P. H. and Smith, J. N.: Estimating nanoparticle growth rates
1092 from size-dependent charged fractions: Analysis of new particle formation events in Mexico City, *J.*
1093 *Geophys. Res. Atmos.*, 113(5), 1–15, doi:10.1029/2007JD009260, 2008.
1094
1095 Järvi, L., Hannuniemi, H., Hussein, T., Junninen, H., Aalto, P., Hillamo, R., Mäkelä, T., Keronen, P.
1096 and Siivola, E.: The urban measurement station SMEAR III : Continuous monitoring of air pollution
1097 and surface – atmosphere interactions in Helsinki , Finland, 14(April), 86–109, 2009.
1098
1099 Jayaratne, R., Pushpawela, B., He, C., Li, H., Gao, J., Chai, F. and Morawska, L.: Observations of
1100 particles at their formation sizes in Beijing, China, *Atmos. Chem. Phys.*, 17(14), 8825–8835,
1101 doi:10.5194/acp-17-8825-2017, 2017.
1102
1103 Jeong, C.-H. H., Evans, G. J., McGuire, M. L., Y.-W. Chang, R., Abbatt, J. P. D. D., Zeromskiene,
1104 K., Mozurkewich, M., Li, S.-M. M., Leaitch, W. R., Chang, R. Y.-W., Abbatt, J. P. D. D.,
1105 Zeromskiene, K., Mozurkewich, M., Li, S.-M. M. and Leaitch, W. R.: Particle formation and growth
1106 at five rural and urban sites, *Atmos. Chem. Phys.*, 10(16), 7979–7995, doi:10.5194/acp-10-7979-
1107 2010, 2010.
1108
1109 Jung, J. G., Pandis, S. N., and Adams, P. J., Evaluation of nucleation theories in a sulfur-rich
1110 environment, *Aerosol Sci. Technol.*, 42, 495–504, doi:10.1080/02786820802187085, 2008.
1111
1112 Jung, J., Adams P. J., and Pandis, S. N., Simulating the size distribution and chemical composition
1113 of ultrafine particles during nucleation events, *Atmos. Environ.*, 40, 2248–2259,
1114 doi:10.1016/j.atmosenv.2005.09.082, 2006.
1115
1116 Kalivitis, N., Kerminen, V.-M., Kouvarakis, G., Stavroulas, I., Tzitzikalaki, E., Kalkavouras, P.,
1117 Daskalakis, N., Myriokefalitakis, S., Bougatioti, A., Manninen, H. E., Roldin, P., Petäjä, T., Boy,
1118 M., Kulmala, M., Kanakidou, M. and Mihalopoulos N.: Formation and growth of atmospheric
1119 nanoparticles in the eastern Mediterranean: Results from long-term measurements and process

1120 simulations', *Atmospheric Chemistry and Physics Discussions*, pp. 1–38. doi: 10.5194/acp-2018-
1121 229, 2019.

1122

1123 Kalkavouras, P., Bossioli, E., Bezantakos, S., Bougiatioti, A., Kalivitis, N., Stavroulas, I.,
1124 Kouvarakis, G., Protonotariou, A. P., Dandou, A., Biskos, G., Mihalopoulos, N., Nenes, A. and
1125 Tombrou, M.: New particle formation in the southern Aegean Sea during the Etesians: Importance
1126 for CCN production and cloud droplet number, *Atmos. Chem. Phys.*, 17(1), 175–192,
1127 doi:10.5194/acp-17-175-2017, 2017.

1128

1129 Kerminen, V., Lehtinen, K. E. J., Anttila, T., Kulmala, M., Lehtinen, K. E. J., Anttila, T. and Kulmala,
1130 M.: Dynamics of atmospheric nucleation mode particles : a timescale analysis, *Tellus*, 56B, 135–146,
1131 doi:10.3402/tellusb.v56i2.16411, 2004.

1132

1133 Kerminen, V. M., Pirjola, L. and Kulmala, M.: How significantly does coagulation scavenging limit
1134 atmospheric particle production?, *J. Geophys. Res. Atmos.*, 106(D20), 24119–24125,
1135 doi:10.1029/2001JD000322, 2001.

1136

1137 Kerminen, V. M., Kulmala, M., Worsnop, D. R., Wildt, J. and Mentel, T. F.: A large source of low-
1138 volatility secondary organic aerosol, *Nature*, 506(7489), 476–479, doi:10.1038/nature13032, 2014.

1139

1140 Ketzel, M., Wählén, P., Kristensson, A., Swietlicki, E., Berkowicz, R., Nielsen, O. J. and Palmgren,
1141 F.: Particle size distribution and particle mass measurements at urban, near-city and rural level in the
1142 Copenhagen area and Southern Sweden, *Atmos. Chem. Phys. Discuss.*, 3(6), 5513–5546,
1143 doi:10.5194/acpd-3-5513-2003, 2004.

1144

1145 Kiendler-Scharr, A., Wildt, J., Dal Maso, M., Hohaus, T., Kleist, E., Mentel, T. F., Tillmann, R.,
1146 Uerlings, R., Schurr, U. and Wahner, A.: New particle formation in forests inhibited by isoprene
1147 emissions, 461, 381–384, 2009.

1148

1149 Kim, K. H., Kabir, E. and Kabir, S.: A review on the human health impact of airborne particulate
1150 matter, *Environ. Int.*, 74, 136–143, doi:10.1016/j.envint.2014.10.005, 2015.

1151

1152 Kirkby, J., Curtius, J., Almeida, J., Dunne, E., Duplissy, J., Ehrhart, S., Franchin, A., Gagné, S., Ickes,
1153 L., Kürten, A., Kupc, A., Metzger, A., Riccobono, F., Rondo, L., Schobesberger, S., Tsagkogeorgas,
1154 G., Wimmer, D., Amorim, A., Bianchi, F., Breitenlechner, M., David, A., Dommen, J., Downard, A.,
1155 Ehn, M., Flagan, R. C., Haider, S., Hansel, A., Hauser, D., Jud, W., Junninen, H., Kreissl, F., Kvashin,
1156 A., Laaksonen, A., Lehtipalo, K., Lima, J., Lovejoy, E. R., Makhmutov, V., Mathot, S., Mikkilä, J.,
1157 Minginette, P., Mogo, S., Nieminen, T., Onnela, A., Pereira, P., Petäjä, T., Schnitzhofer, R., Seinfeld,
1158 J. H., Sipilä, M., Stozhkov, Y., Stratmann, F., Tomé, A., Vanhanen, J., Viisanen, Y., Vrtala, A.,
1159 Wagner, P. E., Walther, H., Weingartner, E., Wex, H., Winkler, P. M., Carslaw, K. S., Worsnop, D.

1160 R., Baltensperger, U. and Kulmala, M.: Role of sulphuric acid, ammonia and galactic cosmic rays in
1161 atmospheric aerosol nucleation, *Nature*, 476(7361), 429–435, doi:10.1038/nature10343, 2011.
1162

1163 Korhonen, P., Kulmala, M., Laaksonen, A., Viisanen, Y., Mcgraw, R. and Seinfeld, J. H.: Ternary
1164 nucleation of H₂SO₄, NH₃ and H₂O in the atmosphere, *J. Geophys. Res.*, 104(D21), 26349–26353,
1165 1999.
1166

1167 Kulmala, M., Petäjä, T., Mönkkönen, P., Koponen, I. K., Dal Maso, M., Aalto, P. P., Lehtinen, K.
1168 E. J. and Kerminen, V.-M.: On the growth of nucleation mode particles: source rates of condensable
1169 vapor in polluted and clean environments, *Atmos. Chem. Phys. Discuss.*, 4(5), 6943–6966,
1170 doi:10.5194/acpd-4-6943-2004, 2005.
1171

1172 Kulmala, M. and Kerminen, V. M.: On the formation and growth of atmospheric nanoparticles,
1173 *Atmos. Res.*, 90(2–4), 132–150, doi:10.1016/j.atmosres.2008.01.005, 2008.
1174

1175 Kulmala, M., Kerminen, V.-M. M., Petäjä, T., Ding, A. J. and Wang, L.: Atmospheric gas-to-particle
1176 conversion: Why NPF events are observed in megacities?, *Faraday Discuss.*, 200, 271–288,
1177 doi:10.1039/c6fd00257a, 2017.
1178

1179 Kulmala, M., Petäjä, T., Nieminen, T., Sipilä, M., Manninen, H. E., Lehtipalo, K., Dal Maso, M.,
1180 Aalto, P. P., Junninen, H., Paasonen, P., Riipinen, I., Lehtinen, K. E. J., Laaksonen, A. and Kerminen,
1181 V. M.: Measurement of the nucleation of atmospheric aerosol particles, *Nat. Protoc.*, 7(9), 1651–
1182 1667, doi:10.1038/nprot.2012.091, 2012.
1183

1184 Kulmala, M., Petäjä, T., Mönkkönen, P., Koponen, I. K., Dal Maso, M., Aalto, P. P., Lehtinen, K. E.
1185 J. and Kerminen, V.-M.: On the growth of nucleation mode particles: source rates of condensable
1186 vapor in polluted and clean environments, *Atmos. Chem. Phys. Discuss.*, 4(5), 6943–6966,
1187 doi:10.5194/acpd-4-6943-2004, 2005.
1188

1189 Kulmala, M., Dal Maso, M., Mäkelä, J. M., Pirjola, L., Väkevä, M., Aalto, P., Miiikkulainen, P.,
1190 Hämeri, K. and O’Dowd, C. D.: On the formation, growth and composition of nucleation mode
1191 particles, *Tellus, Ser. B Chem. Phys. Meteorol.*, 53(4), 479–490, doi:10.3402/tellusb.v53i4.16622,
1192 2001.
1193

1194 Kürten, A., Li, C., Bianchi, F., Curtius, J., Dias, A., Donahue, N. M., Duplissy, J., Flagan, R. C.,
1195 Hakala, J., Jokinen, T., Kirkby, J., Kulmala, M., Laaksonen, A., Lehtipalo, K., Makhmutov, V.,
1196 Onnela, A., Rissanen, M. P., Simon, M., Sipilä, M., Stozhkov, Y., Tröstl, J., Ye, P., and McMurry, P.
1197 H.: New particle formation in the sulfuric acid–dimethylamine–water system: reevaluation of
1198 CLOUD chamber measurements and comparison to an aerosol nucleation and growth model, *Atmos.*
1199 *Chem. Phys.*, 18, 845–863, <https://doi.org/10.5194/acp-18-845-2018>, 2018.

1200 Kürten, A., Bergen, A., Heinritzi, M., Leiminger, M., Lorenz, V., Piel, F., Simon, M., Sitals, R.,
1201 Wagner, A. C. and Curtius, J.: Observation of new particle formation and measurement of sulfuric
1202 acid, ammonia, amines and highly oxidized organic molecules at a rural site in central Germany,
1203 *Atmos. Chem. Phys.*, 16(19), 12793–12813, doi:10.5194/acp-16-12793-2016, 2016.
1204
1205 Lee, S.-H. H., Uin, J., Guenther, A. B., de Gouw, J. A., Yu, F., Nadykto, A. B., Herb, J., Ng, N. L.,
1206 Koss, A., Brune, W. H., Baumann, K., Kanawade, V. P., Keutsch, F. N., Nenes, A., Olsen, K.,
1207 Goldstein, A. and Ouyang, Q.: Isoprene suppression of new particle formation: Potential
1208 mechanisms and implications, *J. Geophys. Res. Atmos.*, 121(24), 14,621–14,635,
1209 doi:10.1002/2016JD024844, 2016.
1210
1211 Lehtinen, K. E. J., Korhonen, H., Dal Maso, M. and Kulmala, M.: On the concept of condensation
1212 sink diameter, *Boreal Environ. Res.*, 8(4), 405–411, 2003.
1213
1214 Lehtipalo, K., Yan, C., Dada, L., Bianchi, F., Xiao, M., Wagner, R., Stolzenburg, D., Ahonen, L. R.,
1215 Amorim, A., Baccharini, A., Bauer, P. S., Baumgartner, B., Bergen, A., Bernhammer, A.,
1216 Breitenlechner, M., Brilke, S., Buchholz, A., Mazon, S. B., Chen, D., Chen, X., Dias, A., Dommen,
1217 J., Draper, D. C., Duplissy, J., Ehn, M., Finkenzeller, H., Fischer, L., Frege, C., Fuchs, C., Garmash,
1218 O., Gordon, H., Hakala, J., He, X., Heikkinen, L., Heinritzi, M., Helm, J. C., Hofbauer, V., Hoyle, C.
1219 R., Jokinen, T., Ojdanic, A., Onnela, A., Passananti, M., Petäjä, T., Piel, F., Sarnela, N., Schallhart,
1220 S., Schuchmann, S., Sengupta, K. and Simon, M.: Multicomponent new particle formation from
1221 sulfuric acid, ammonia, and biogenic vapors, (3), 1–10, 2018.
1222
1223 Li, X., Chee, S., Hao, J., Abbatt, J. P. D., Jiang, J. and Smith, J. N.: Relative humidity effect on the
1224 formation of highly oxidized molecules and new particles during monoterpene oxidation, *Atmos.*
1225 *Chem. Phys.*, 19(3), 1555–1570, doi:10.5194/acp-19-1555-2019, 2019.
1226
1227 Makkonen, R., Asmi, A., Kerminen, V. M., Boy, M., Arneth, A., Hari, P. and Kulmala, M.: Air
1228 pollution control and decreasing new particle formation lead to strong climate warming, *Atmos.*
1229 *Chem. Phys.*, 12(3), 1515–1524, doi:10.5194/acp-12-1515-2012, 2012.
1230
1231 McFiggans, G., Mentel, T. F., Wildt, J., Pullinen, I., Kang, S., Kleist, E., Schmitt, S., Springer, M.,
1232 Tillmann, R., Wu, C., Zhao, D., Hallquist, M., Faxon, C., Le Breton, M., Hallquist, Å. M., Simpson,
1233 D., Bergström, R., Jenkin, M. E., Ehn, M., Thornton, J. A., Alfarra, M. R., Bannan, T. J., Percival, C.
1234 J., Priestley, M., Topping, D. and Kiendler-Scharr, A.: Secondary organic aerosol reduced by mixture
1235 of atmospheric vapours, *Nature*, 565(7741), 587–593, doi:10.1038/s41586-018-0871-y, 2019.
1236 Merikanto, J., Spracklen, D. V., Mann, G. W., Pickering, S. J. and Carslaw, K. S.: Impact of
1237 nucleation on global CCN, *Atmos. Chem. Phys.*, 9(21), 8601–8616, doi:10.5194/acp-9-8601-2009,
1238 2009.
1239

1240 Merikanto, J., Spracklen, D. V., Mann, G. W., Pickering, S. J. and Carslaw, K. S.: Impact of
1241 nucleation on global CCN, *Atmos. Chem. Phys.*, 9(21), 8601–8616, doi:10.5194/acp-9-8601-2009,
1242 2009.
1243
1244 Metzger, A., Verheggen, B., Dommen, J., Duplissy, J., Prevot, A. S. H., Weingartner, E., Riipinen,
1245 I., Kulmala, M., Spracklen, D. V., Carslaw, K. S. and Baltensperger, U.: Evidence for the role of
1246 organics in aerosol particle formation under atmospheric conditions, *Proc. Nat. Acad. Sci.*, 107(15),
1247 6646–6651, doi:10.1073/pnas.0911330107, 2010.
1248
1249 Minguillón, M. C., Brines, M., Pérez, N., Reche, C., Pandolfi, M., Fonseca, A. S., Amato, F.,
1250 Alastuey, A., Lyasota, A., Codina, B., Lee, H. K., Eun, H. R., Ahn, K. H. and Querol, X.: New particle
1251 formation at ground level and in the vertical column over the Barcelona area, *Atmos. Res.*, 164–165,
1252 118–130, doi:10.1016/j.atmosres.2015.05.003, 2015.
1253
1254 Mirabel, P. and Katz, J. L.: Binary homogeneous nucleation as a mechanism for the formation of
1255 aerosols, *J. Chem. Phys.*, 60(3), 1138–1144, doi:10.1063/1.1681124, 1974.
1256
1257 Mølgaard, B., Birmili, W., Clifford, S., Massling, A., Eleftheriadis, K., Norman, M., Vratolis, S.,
1258 Wehner, B., Corander, J., Hämeri, K. and Hussein, T.: Evaluation of a statistical forecast model for
1259 size-fractionated urban particle number concentrations using data from five European cities, *J.*
1260 *Aerosol Sci.*, 66, 96–110, doi:10.1016/j.jaerosci.2013.08.012, 2013.
1261
1262 Molteni, U., Bianchi, F., Klein, F., El Haddad, I., Frege, C., Rossi, M. J., Dommen, J. and
1263 Baltensperger, U.: Formation of highly oxygenated organic molecules from aromatic compounds,
1264 *Atmos. Chem. Phys.*, 18(3), 1909–1921, doi:10.5194/acp-18-1909-2018, 2018.
1265
1266 Napari, I., Noppel, M., Vehkamäki, H. and Kulmala, M.: An improved model for ternary nucleation
1267 of sulfuric acid-ammonia-water, *J. Chem. Phys.*, 116(10), 4221–4227, doi:10.1063/1.1450557, 2002.
1268
1269 Nieminen, T., Kerminen, V.-M., Petäjä, T., Aalto, P. P., Arshinov, M., Asmi, E., Baltensperger, U.,
1270 Beddows, D. C. S., Beukes, J. P., Collins, D., Ding, A., Harrison, R. M., Henzing, B., Hooda, R., Hu,
1271 M., Hörrak, U., Kivekäs, N., Komsaare, K., Krejci, R., Kristensson, A., Laakso, L., Laaksonen, A.,
1272 Leaitch, W. R., Lihavainen, H., Mihalopoulos, N., Németh, Z., Nie, W., O ’dowd, C., Salma, I.,
1273 Sellegri, K., Svenningsson, B., Swietlicki, E., Tunved, P., Ulevicius, V., Vakkari, V., Vana, M.,
1274 Wiedensohler, A., Wu, Z., Virtanen, A., Kulmala, M., O’Dowd, C., Salma, I., Sellegri,
1275 K., Svenningsson, B., Swietlicki, E., Tunved, P., Ulevicius, V., Vakkari, V., Vana, M., Wiedensohler,
1276 A., Wu, Z., Virtanen, A., Kulmala, M., O ’dowd, C., Salma, I., Sellegri, K., Svenningsson, B.,
1277 Swietlicki, E., Tunved, P., Ulevicius, V., Vakkari, V., Vana, M., Wiedensohler, A., Wu, Z., Virtanen,
1278 A. and Kulmala, M.: Global analysis of continental boundary layer new particle formation based on
1279 long-term measurements, *Atmos. Chem. Phys. Discuss*, 5194, 2018–304, doi:10.5194/acp-2018-304,

1280 2018.
1281
1282 Nieminen, T., Lehtinen, K. E. J. and Kulmala, M.: Sub-10 nm particle growth by vapor condensation-
1283 effects of vapor molecule size and particle thermal speed, *Atmos. Chem. Phys.*, 10(20), 9773–9779,
1284 doi:10.5194/acp-10-9773-2010, 2010.
1285
1286 O’Dowd, C. D., Jimenez, J. L., Bahreini, R., Flagan, R. C., Seinfeld, J. H., Hameri Kaarle, Pirjola,
1287 L., Kulmala, M., Jennings, S. G. and Hoffmann, T.: Marine aerosol formation from biogenic iodine
1288 emissions, *Lett. to Nat.*, 417(June), 1–5, doi:10.1038/nature00773.1.2.3.4.5.6.7.8.9.10., 2002.
1289
1290 Olenius, T., Halonen, R., Kurten, T., Henschel, H., Maatta, O. K., Ortega, I. K., Jen, C.,
1291 Vehkamäki, H. and Riipinen, I.: New particle formation from sulfuric acid amines: Comparison of
1292 monomethylamine, dimethylamine, and trimethylamine, *J. Geophys. Res. Atmos.*, 7103–7118,
1293 doi:10.1002/2017JD026501, 2017.
1294
1295 Olin, M., Kuuluvainen, H., Aurela, M., Kalliokoski, J., Kuittinen, N., Isotalo, M., Timonen, H. J.,
1296 Niemi, J. V., Rönkkö, T., and Dal Maso, M.: Traffic-originated nanocluster emission exceeds
1297 H₂SO₄-driven photochemical new particle formation in an urban area, *Atmos. Chem. Phys.*, 20, 1–
1298 13, <https://doi.org/10.5194/acp-20-1-2020>, 2020.
1299
1300 Paasonen, P., Asmi, A., Petäjä, T., Kajos, M. K., Äijälä, M., Junninen, H., Holst, T., Abbatt, J. P.
1301 D., Arneth, A., Birmili, W., Van Der Gon, H. D., Hamed, A., Hoffer, A., Laakso, L., Laaksonen,
1302 A., Richard Leitch, W., Plass-Dülmer, C., Pryor, S. C., Räisänen, P., Swietlicki, E., Wiedensohler,
1303 A., Worsnop, D. R., Kerminen, V. M. and Kulmala, M.: Warming-induced increase in aerosol
1304 number concentration likely to moderate climate change, *Nat. Geosci.*, 6(6), 438–442,
1305 doi:10.1038/ngeo1800, 2013.
1306
1307 Park, M., Yum, S. S. and Kim, J. H.: Characteristics of submicron aerosol number size distribution
1308 and new particle formation events measured in Seoul, Korea, during 2004–2012, *Asia-Pacific J.*
1309 *Atmos. Sci.*, 51(1), 1–10, doi:10.1007/s13143-014-0055-0, 2015.
1310
1311 Petäjä, T., Mauldin, R. L., Kosciuch, E., McGrath, J., Nieminen, T., Paasonen, P., Boy, M.,
1312 Adamov, A., Kotiaho, T. and Kulmala, M.: Sulfuric acid and OH concentrations in a boreal forest
1313 site, *Atmos. Chem. Phys.*, 9(19), 7435–7448, doi:10.5194/acp-9-7435-2009, 2009.
1314
1315 Pikridas, M., Sciare, J., Freutel, F., Crumeyrolle, S., Von Der Weiden-Reinmüller, S. L., Borbon, A.,
1316 Schwarzenboeck, A., Merkel, M., Crippa, M., Kostenidou, E., Psychoudaki, M., Hildebrandt, L.,
1317 Engelhart, G. J., Petäjä, T., Prévôt, A. S. H., Drewnick, F., Baltensperger, U., Wiedensohler, A.,
1318 Kulmala, M., Beekmann, M. and Pandis, S. N.: In situ formation and spatial variability of particle
1319 number concentration in a European megacity, *Atmos. Chem. Phys.*, 15(17), 10219–10237,

1320 doi:10.5194/acp-15-10219-2015, 2015.
1321
1322 Pillai, P., Khlystov, A., Walker, J. and Aneja, V.: Observation and analysis of particle nucleation at
1323 a forest site in southeastern US, *Atmosphere (Basel)*, 4(2), 72–93, doi:10.3390/atmos4020072, 2013.
1324
1325 Poling, B. E., Prausnitz, J. M. and O’Connell, J. P.: *The properties of gases and liquids*, 5th ed.,
1326 McGraw-Hill Education., 2001.
1327
1328 Politis, M., Pilinis, C. and Lekkas, T. D.: Ultrafine particles (UFP) and health effects. Dangerous.
1329 Like no other PM? Review and analysis, *Glob. Nest J.*, 10(3), 439–452, 2008.
1330
1331 Quéléver, L. L. J., Kristensen, K., Normann Jensen, L., Rosati, B., Teiwes, R., Daellenbach, K. R.,
1332 Peräkylä, O., Roldin, P., Bossi, R., Pedersen, H. B., Glasius, M., Bilde, M. and Ehn, M.: Effect of
1333 temperature on the formation of highly oxygenated organic molecules (HOMs) from alpha-pinene
1334 ozonolysis, *Atmos. Chem. Phys.*, 19(11), 7609–7625, doi:10.5194/acp-19-7609-2019, 2019.
1335
1336 Querol, X., Gangoiti, G., Mantilla, E., Alastuey, A., Minguillón, M. C., Amato, F., Reche, C., Viana,
1337 M., Moreno, T., Karanasiou, A., Rivas, I., Pérez, N., Ripoll, A., Brines, M., Ealo, M., Pandolfi, M.,
1338 Lee, H. K., Eun, H. R., Park, Y. H., Escudero, M., Beddows, D., Harrison, R. M., Bertrand, A.,
1339 Marchand, N., Lyasota, A., Codina, B., Olid, M., Udina, M., Jiménez-Esteve, B. B., Jiménez-Esteve,
1340 B. B., Alonso, L., Millán, M. and Ahn, K. H.: Phenomenology of high-ozone episodes in NE Spain,
1341 *Atmos. Chem. Phys.*, 17(4), 2817–2838, doi:10.5194/acp-17-2817-2017, 2017.
1342
1343 Riccobono, F., Schobesberger, S., Scott, C. E., Dommen, J., Ortega, I. K., Rondo, L., Almeida, J.,
1344 Amorim, A., Bianchi, F., Breitenlechner, M., David, A., Downard, A., Dunne, E. M., Duplissy, J.,
1345 Ehrhart, S., Flagan, R. C., Franchin, A., Hansel, A., Junninen, H., Kajos, M., Keskinen, H., Kupc, A.,
1346 Makhmutov, V., Mathot, S., Nieminen, T., Onnela, A., Petäjä, T., Tsagkogeorgas, G., Vaattovaara,
1347 P., Viisanen, Y., Vrtala, A. and Wagner, P. E.: Oxidation Products of biogenic atmospheric particles,
1348 *Science*, 717, 717–722, doi:10.1126/science.1243527, 2014.
1349
1350 Rimnácová, D., Ždímal, V., Schwarz, J., Smolík, J. and Rimnác, M.: Atmospheric aerosols in suburb
1351 of Prague: The dynamics of particle size distributions, *Atmos. Res.*, 101(3), 539–552,
1352 doi:10.1016/j.atmosres.2010.10.024, 2011.
1353 Rose, C., Zha, Q., Dada, L., Yan, C., Lehtipalo, K., Junninen, H., Mazon, S. B., Jokinen, T., Sarnela,
1354 N., Sipilä, M., Petäjä, T., Kerminen, V. M., Bianchi, F. and Kulmala, M.: Observations of biogenic
1355 ion-induced cluster formation in the atmosphere, *Sci. Adv.*, 4(4), 1–10, doi:10.1126/sciadv.aar5218,
1356 2018.
1357
1358 Rivas, I., Beddows, D. C. S., Amato, F., Green, D. C., Järvi, L., Hueglin, C., Reche, C., Timonen, H.,
1359 Fuller, G. W., Niemi, J. V, Pérez, N., Aurela, M., Hopke, P. K., Alastuey, A., Kulmala, M., Harrison,

1360 R. M., Querol, X. and Kelly, F. J.: Source apportionment of particle number size distribution in urban
1361 background and traffic stations in four European cities, *Environ. Int.*, 135, 105345,
1362 doi:10.1016/j.envint.2019.105345, 2020.

1363

1364 Rizzo, L. V., Artaxo, P., Karl, T., Guenther, A. B. and Greenberg, J.: Aerosol properties, in-canopy
1365 gradients, turbulent fluxes and VOC concentrations at a pristine forest site in Amazonia, *Atmos.*
1366 *Environ.*, 44(4), 503–511, doi:10.1016/j.atmosenv.2009.11.002, 2010.

1367

1368 Salma, I., Borsòs, T., Weidinger, T., Aalto, P., Hussein, T., Dal Maso, M. and Kulmala, M.:
1369 Production, growth and properties of ultrafine atmospheric aerosol particles in an urban environment,
1370 *Atmos. Chem. Phys.*, 11(3), 1339–1353, doi:10.5194/acp-11-1339-2011, 2011.

1371

1372 Schwartz, J., Dockery, D. W. and Neas, L. M.: Is Daily Mortality Associated Specifically with Fine
1373 Particles?, *J. Air Waste Manag. Assoc.*, 46(10), 927–939, doi:10.1080/10473289.1996.10467528,
1374 1996.

1375

1376 Seinfeld, J. H. and Pandis, S. N.: *Atmospheric Chemistry and Physics: From Air Pollution to Climate*
1377 *Change*, 3rd Editio., John Wiley & Sons, Inc, New Jersey, Canada, 2012.

1378

1379 Shen, X., Sun, J., Kivekäs, N., Kristensson, A., Zhang, X., Zhang, Y., Zhang, L., Fan, R., Qi, X., Ma,
1380 Q. and Zhou, H.: Spatial distribution and occurrence probability of regional new particle formation
1381 events in eastern China, *Atmos. Chem. Phys.*, 18(2), 587–599, doi:10.5194/acp-18-587-2018, 2018.

1382

1383 Shrivastava, M., Cappa, C. D., Fan, J., Goldstein, A. H., Guenther, A. B., Jimenez, J. L., Kuang, C.,
1384 Laskin, A., Martin, S. T., Ng, N. L., Petaja, T., Pierce, J. R., Rasch, P. J., Roldin, P., Seinfeld, J. H.,
1385 Shilling, J., Smith, J. N., Thornton, J. A., Volkamer, R., Wang, J., Worsnop, D. R., Zaveri, R. A.,
1386 Zelenyuk, A. and Zhang, Q.: Recent advances in understanding secondary organic aerosol:
1387 Implications for global climate forcing, *Rev. Geophys.*, 55(2), 509–559,
1388 doi:10.1002/2016RG000540, 2017.

1389

1390 Siakavaras, D., Samara, C., Petrakakis, M. and Biskos, G.: Nucleation events at a coastal city during
1391 the warm period: Kerbside versus urban background measurements, *Atmos. Environ.*, 140, 60–68,
1392 doi:10.1016/j.atmosenv.2016.05.054, 2016.

1393

1394 Sipila, M., Berndt, T., Petaja, T., Brus, D., Vanhanen, J., Stratmann, F., Patokoski, J., Mauldin III,
1395 R. L., Hyvarinen, A. P., Lihavainen, H. and Kulmala, M.: The Role of Sulfuric Acid in
1396 Atmospheric Nucleation, *Science*, 327, 1243–1246, doi:10.1126/science.1180315, 2010.

1397

1398 Spracklen, D. V., Carslaw, K. S., Merikanto, J., Mann, G. W., Reddington, C. L., Pickering, S., Ogren,
1399 J. A., Andrews, E., Baltensperger, U., Weingartner, E., Boy, M., Kulmala, M., Laakso, L.,

1400 Lihavainen, H., Kivekäs, N., Komppula, M., Mihalopoulos, N., Kouvarakis, G., Jennings, S. G.,
1401 O'Dowd, C., Birmili, W., Wiedensohler, A., Weller, R., Gras, J., Laj, P., Sellegri, K., Bonn, B.,
1402 Krejci, R., Laaksonen, A., Hamed, A., Minikin, A., Harrison, R. M., Talbot, R. and Sun, J.: Explaining
1403 global surface aerosol number concentrations in terms of primary emissions and particle formation,
1404 *Atmos. Chem. Phys.*, 10(10), 4775–4793, doi:10.5194/acp-10-4775-2010, 2010.
1405
1406 Stolzenburg, D., Simon, M., Ranjithkumar, A., Kürten, A., Lehtipalo, K., Gordon, H., Ehrhart, S.,
1407 Finkenzeller, H., Pichelstorfer, L., Nieminen, T., He, X.-C., Brilke, S., Xiao, M., Amorim, A.,
1408 Baalbaki, R., Baccarini, A., Beck, L., Bräkling, S., Caudillo Murillo, L., Chen, D., Chu, B., Dada,
1409 L., Dias, A., Dommen, J., Duplissy, J., El Haddad, I., Fischer, L., Gonzalez Carracedo, L., Heinritzi,
1410 M., Kim, C., Koenig, T. K., Kong, W., Lamkaddam, H., Lee, C. P., Leiminger, M., Li, Z.,
1411 Makhmutov, V., Manninen, H. E., Marie, G., Marten, R., Müller, T., Nie, W., Partoll, E., Petäjä, T.,
1412 Pfeifer, J., Philippov, M., Rissanen, M. P., Rörup, B., Schobesberger, S., Schuchmann, S., Shen, J.,
1413 Sipilä, M., Steiner, G., Stozhkov, Y., Tauber, C., Tham, Y. J., Tomé, A., Vazquez-Pufleau, M.,
1414 Wagner, A. C., Wang, M., Wang, Y., Weber, S. K., Wimmer, D., Wlasits, P. J., Wu, Y., Ye, Q.,
1415 Zauner-Wieczorek, M., Baltensperger, U., Carslaw, K. S., Curtius, J., Donahue, N. M., Flagan, R.
1416 C., Hansel, A., Kulmala, M., Lelieveld, J., Volkamer, R., Kirkby, J., and Winkler, P. M.: Enhanced
1417 growth rate of atmospheric particles from sulfuric acid, *Atmos. Chem. Phys.*, 20, 7359–7372,
1418 <https://doi.org/10.5194/acp-20-7359-2020>, 2020.
1419
1420 Stolzenburg, D., Fischer, L., Vogel, A. L., Heinritzi, M., Schervish, M. and Simon, M., Wagner, A.
1421 C., Dada, L., Ahonen, L. R., Amorim, A., Baccarini, A., Bauer, P. S., Baumgartner, B., Bergen, A.,
1422 Bianchi, F., Breitenlechner, M., Brilke, S., Buenorstro Mazon, S., Chen, D., Dias, A., Draper, D. C.,
1423 Duplissy, J., El Haddad, I., Finkenzeller, H., Frege, C., Fuchs, C., Garmash, O., Gordon, H., He, X.,
1424 Helm, J., Hofbauer, V., Hoyle, C. R., Kim, C., Kirkby, J., Kontkanen, J., Kürten, A., Lampilahti, J.,
1425 Lawler, M., Lehtipalo, K., Leiminger, M., Mai, H., Mathot, S., Mentler, B., Molteni, U., Nie, W.,
1426 Nieminen, T., Nowak, J. B., Ojdanic, A., Onnela, A., Passananti, M., Petäjä, T., Quéléver, L. L. J.,
1427 Rissanen, M. P., Sarnela, N., Schallhart, S., Tauber, C., Tome, A., Wagner, R., Wang, M., Weitz,
1428 L., Wimmer, D., Xiao, M., Yan, C., Ye, P., Zha, Q., Baltensperger, U., Curtius, J., Dommen, J.,
1429 Flagan, R. C., Kulmala, M., Smith, J. N., Worsnop, D. R., Hansel, A., Donahue, N. M., Winkler, P.
1430 M.: Rapid growth of organic aerosol nanoparticles over a wide tropospheric temperature range,
1431 *PNAS*, 115(37), doi:10.1073/pnas.1807604115, 2018.
1432
1433 Tröstl, J., Chuang, W. K., Gordon, H., Heinritzi, M., Yan, C., Molteni, U., Ahlm, L., Frege, C.,
1434 Bianchi, F., Wagner, R., Simon, M., Lehtipalo, K., Williamson, C., Craven, J. S., Duplissy, J.,
1435 Adamov, A., Almeida, J., Bernhammer, A. K., Breitenlechner, M., Brilke, S., Dias, A., Ehrhart, S.,
1436 Flagan, R. C., Franchin, A., Fuchs, C., Guida, R., Gysel, M., Hansel, A., Hoyle, C. R., Jokinen, T.,
1437 Junninen, H., Kangasluoma, J., Keskinen, H., Kim, J., Krapf, M., Kürten, A., Laaksonen, A., Lawler,
1438 M., Leiminger, M., Mathot, S., Möhler, O., Nieminen, T., Onnela, A., Petäjä, T., Piel, F. M.,
1439 Miettinen, P., Rissanen, M. P., Rondo, L., Sarnela, N., Schobesberger, S., Sengupta, K., Sipilä, M.,

1440 Smith, J. N., Steiner, G., Tomè, A., Virtanen, A., Wagner, A. C., Weingartner, E., Wimmer, D.,
1441 Winkler, P. M., Ye, P., Carslaw, K. S., Curtius, J., Dommen, J., Kirkby, J., Kulmala, M., Riipinen, I.,
1442 Worsnop, D. R., Donahue, N. M. and Baltensperger, U.: The role of low-volatility organic compounds
1443 in initial particle growth in the atmosphere, *Nature*, 533(7604), 527–531, doi:10.1038/nature18271,
1444 2016.
1445
1446 Vratolis, S., Gini, M. I., Bezantakos, S., Stavroulas, I., Kalivitis, N., Kostenidou, E., Louvaris, E.,
1447 Siakavaras, D., Biskos, G., Mihalopoulos, N., Pandis, S. N. N., Pilinis, C., Papayannis, A. and
1448 Eleftheriadis, K.: Particle number size distribution statistics at City-Centre Urban Background, urban
1449 background, and remote stations in Greece during summer, *Atmos. Environ.*, 213(May), 711–726,
1450 doi:10.1016/j.atmosenv.2019.05.064, 2019.
1451
1452 von Bismarck-Osten, C., Birmili, W., Ketznel, M. and Weber, S.: Statistical modelling of aerosol
1453 particle number size distributions in urban and rural environments - A multi-site study, *Urban*
1454 *Climate*, 11(C), pp. 51–66. doi: 10.1016/j.uclim.2014.11.004, 2015.
1455
1456 von Bismarck-Osten, C. and Weber, S.: A uniform classification of aerosol signature size
1457 distributions based on regression-guided and observational cluster analysis, *Atmospheric*
1458 *Environment*, 89, pp. 346–357. doi: 10.1016/j.atmosenv.2014.02.050, 2014.
1459
1460 von Bismarck-Osten, C. Birmili, W., Ketznel, M., Massling, A., Petäjä, T. and Weber, S.:
1461 Characterization of parameters influencing the spatio-temporal variability of urban particle number
1462 size distributions in four European cities, *Atmospheric Environment*, 77, pp. 415–429. doi:
1463 10.1016/j.atmosenv.2013.05.029, 2013.
1464
1465 Wagner, P. and Kuttler, W.: Biogenic and anthropogenic isoprene in the near-surface urban
1466 atmosphere - A case study in Essen, Germany, *Sci. Total Environ.*, 475, 104–115,
1467 doi:10.1016/j.scitotenv.2013.12.026, 2014.
1468
1469 Wang, D., Fu, Q., Geng, F., Li, L., Wang, H., Qiao, L., Yang, X., Chen, J., Kerminen, V. M.,
1470 Petäjä, T., Worsnop, D. R., Kulmala, M. and Wang, L.: Atmospheric new particle formation from
1471 sulfuric acid and amines in a Chinese megacity, *Science*, 361(6399), 278–281,
1472 doi:10.1126/science.aao4839, 2018.
1473
1474 Wang, S., Wu, R., Berndt, T., Ehn, M. and Wang, L.: Formation of Highly Oxidized Radicals and
1475 Multifunctional Products from the Atmospheric Oxidation of Alkylbenzenes, ,
1476 doi:10.1021/acs.est.7b02374, 2017a.
1477
1478 Wang, Z., Wu, Z., Yue, D., Shang, D., Guo, S., Sun, J., Ding, A., Wang, L., Jiang, J., Guo, H., Gao,
1479 J., Cheung, H. C., Morawska, L., Keywood, M. and Hu, M.: New particle formation in China: Current

1480 knowledge and further directions, *Sci. Total Environ.*, 577, 258–266,
1481 doi:10.1016/j.scitotenv.2016.10.177, 2017b.
1482
1483 Wang, F., Ketzler, M., Ellermann, T., Wåhlin, P., Jensen, S. S., Fang, D. and Massling, A.: Particle
1484 number, particle mass and NO_x emission factors at a highway and an urban street in Copenhagen,
1485 *Atmos. Chem. Phys.*, 10(6), 2745–2764, doi:10.5194/acp-10-2745-2010, 2010.
1486
1487 Wang, M., Kong, W., Marten, R., He, X. C., Chen, D., Pfeifer, J., Heitto, A., Kontkanen, J., Dada,
1488 L., Kürten, A., Yli-Juuti, T., Manninen, H. E., Amanatidis, S., Amorim, A., Baalbaki, R., Baccarini,
1489 A., Bell, D. M., Bertozzi, B., Bräkling, S., Brilke, S., Murillo, L. C., Chiu, R., Chu, B., De
1490 Menezes, L. P., Duplissy, J., Finkenzeller, H., Carracedo, L. G., Granzin, M., Guida, R., Hansel, A.,
1491 Hofbauer, V., Krechmer, J., Lehtipalo, K., Lamkaddam, H., Lampimäki, M., Lee, C. P.,
1492 Makhmutov, V., Marie, G., Mathot, S., Mauldin, R. L., Mentler, B., Müller, T., Onnela, A., Partoll,
1493 E., Petäjä, T., Philippov, M., Pospisilova, V., Ranjithkumar, A., Rissanen, M., Rörup, B., Scholz,
1494 W., Shen, J., Simon, M., Sipilä, M., Steiner, G., Stolzenburg, D., Tham, Y. J., Tomé, A., Wagner,
1495 A. C., Wang, D. S., Wang, Y., Weber, S. K., Winkler, P. M., Wlasits, P. J., Wu, Y., Xiao, M., Ye,
1496 Q., Zauner-Wieczorek, M., Zhou, X., Volkamer, R., Riipinen, I., Dommen, J., Curtius, J.,
1497 Baltensperger, U., Kulmala, M., Worsnop, D. R., Kirkby, J., Seinfeld, J. H., El-Haddad, I., Flagan,
1498 R. C. and Donahue, N. M.: Rapid growth of new atmospheric particles by nitric acid and ammonia
1499 condensation, *Nature*, 581(7807), 184–189, doi:10.1038/s41586-020-2270-4, 2020.
1500
1501 Weber, R. J., McMurry, P. H., Eisele, F. L. and Tanner, D. J.: Measurement of expected nucleation
1502 precursor species and 3-500-nm diameter particles at Mauna Loa Observatory, Hawaii, *J. Atmos.*
1503 *Sci.*, 52(12), 2242–2257, doi:10.1175/1520-0469(1995)052<2242:MOENPS>2.0.CO;2, 1995.
1504
1505 Wehner, B., Siebert, H., Stratmann, F., Tuch, T., Wiedensohler, A., Petäjä, T., Dal Maso, M. and
1506 Kulmala, M.: Horizontal homogeneity and vertical extent of new particle formation events, *Tellus*,
1507 *Ser. B Chem. Phys. Meteorol.*, 59(3), 362–371, doi:10.1111/j.1600-0889.2007.00260.x, 2007.
1508
1509 Wiedensohler, A., Ma, N., Birmili, W., Heintzenberg, J., Ditas, F., Andreae, M. O. and Panov, A.:
1510 Infrequent new particle formation over the remote boreal forest of Siberia, *Atmos. Environ.*, 200,
1511 167–169, doi:10.1016/j.atmosenv.2018.12.013, 2019.
1512
1513 Wonaschütz, A., Demattio, A., Wagner, R., Burkart, J., Zíková, N., Vodička, P., Ludwig, W., Steiner,
1514 G., Schwarz, J. and Hitzenberger, R.: Seasonality of new particle formation in Vienna, Austria -
1515 Influence of air mass origin and aerosol chemical composition, *Atmos. Environ.*, 118, 118–126,
1516 doi:10.1016/j.atmosenv.2015.07.035, 2015.
1517

1518 Woo, K. S., Chen, D. R., Pui, D. Y. H. H. and McMurry, P. H.: Measurement of Atlanta aerosol
1519 size distributions: Observations of lutrafine particle events, *Aerosol Sci. Technol.*, 34, 75–87,
1520 doi:10.1080/02786820120056, 2001.
1521

1522 Yamada, H.: Contribution of evaporative emissions from gasoline vehicles toward total VOC
1523 emissions in Japan, *Sci. Total Environ.*, 449, 143–149, doi:10.1016/j.scitotenv.2013.01.045, 2013.
1524

1525 Yan, C., Nie, W., Vogel, A. L., Dada, L., Lehtipalo, K., Stolzenburg, D. and Wagner, R.: Size-
1526 dependent influence of NO_x on the growth rates of organic aerosol particles, *Sci. Adv.*, 6, 1–10,
1527 2020.
1528

1529 Yan, C., Dada, L., Rose, C., Jokinen, T., Nie, W., Schobesberger, S., Junninen, H., Lehtipalo, K.,
1530 Sarnela, N., Makkonen, U., Garmash, O., Wang, Y., Zha, Q., Paasonen, P., Bianchi, F., Sipilä, M.,
1531 Ehn, M., Petäjä, T., Kerminen, V.-M., Worsnop, D. R. and Kulmala, M.: The role of H₂SO₄-
1532 NH₃ anion clusters in ion-induced aerosol nucleation mechanisms in the boreal forest, *Atmos.*
1533 *Chem. Phys.*, 18, 13231–13243, doi:10.5194/acp-18-13231-2018, 2018.
1534

1535 Yao, L., Garmash, O., Bianchi, F., Zheng, J., Yan, C., Kontkanen, J., Junninen, H., Mazon, S. B.,
1536 Ehn, M., Paasonen, P., Sipilä, M., Wang, M., Wang, X., Xiao, S., Chen, H., Lu, Y., Zhang, B.,
1537 Wang, M., Chen, D., Xiao, M., Ye, Q., Stolzenburg, D., Hofbauer, V., Ye, P., Vogel, A. L.,
1538 Mauldin, R. L., Amorim, A., Baccarini, A., Baumgartner, B., Brilke, S., Dada, L., Dias, A.,
1539 Duplissy, J., Finkenzeller, H., Garmash, O., He, X. C., Hoyle, C. R., Kim, C., Kvashnin, A.,
1540 Lehtipalo, K., Fischer, L., Molteni, U., Petäjä, T., Pospisilova, V., Quéléver, L. L. J., Rissanen, M.,
1541 Simon, M., Tauber, C., Tomé, A., Wagner, A. C., Weitz, L., Volkamer, R., Winkler, P. M., Kirkby,
1542 J., Worsnop, D. R., Kulmala, M., Baltensperger, U., Dommen, J., El-Haddad, I. and Donahue, N.
1543 M.: Photo-oxidation of Aromatic Hydrocarbons Produces Low-Volatility Organic Compounds,
1544 *Environ. Sci. Technol.*, 54(13), 7911–7921, doi:10.1021/acs.est.0c02100, 2020.
1545

1546 Ye, J., Abbatt, J. P. D., Chan, A. W.H., Novel pathway of SO₂ oxidation in the atmosphere:
1547 reactions with monoterpene ozonolysis intermediates and secondary organic aerosol, *Atmos. Chem.*
1548 *Phys.*, 18, 5549-5565, 2018

1549 Yli-Juuti, T., Mohr, C. and Riipinen, I.: Open questions on atmospheric nanoparticle growth,
1550 *Commun. Chem.*, 3(1), 2–5, doi:10.1038/s42004-020-00339-4, 2020.
1551

1552 Zhang, R., Khalizov, A., Wang, L., Hu, M. and Xu, W.: Nucleation and growth of nanoparticles in
1553 the atmosphere, *Chem. Rev.*, 112(3), 1957–2011, doi:10.1021/cr2001756, 2012.
1554
1555

1556 **TABLE LEGENDS**

1557

1558 **Table 1:** Location and data availability of the sites.

1559

1560 **Table 2:** Frequency (and number of NPF events), growth and formation rate of NPF events.

1561

1562 **Table 3:** Normalised gradients (non-normalised for growth rate), R^2 and p-values (- for values
1563 >0.05) for the relationship between meteorological conditions and NPF event
1564 variables. Gradients of $R^2 > 0.50$ are in bold.

1565

1566 **Table 4:** Normalised gradients (non-normalised for growth rate), R^2 and p-values (- for values
1567 >0.05) for the relationship between atmospheric composition variables and NPF
1568 event variables. Gradients of $R^2 > 0.50$ are in bold.

1569

1570

1571 **FIGURE LEGENDS**

1572

1573 **Figure 1:** Map of the sites of the present study.

1574

1575 **Figure 2:** Relation of average downward incoming solar radiation (K_{\downarrow}) and normalised
1576 gradients a_N^* .

1577

1578 **Figure 3:** Normalised gradients a_J^* for K_{\downarrow} (*UK sites are calculated with solar irradiance).

1579

1580 **Figure 4:** Relationship of average relative humidity and normalised gradients a_N^* .

1581

1582 **Figure 5:** Relationship of average temperature and normalised gradients a_N^* .

1583

1584 **Figure 6:** Normalised gradients a_J^* for temperature.

1585

1586 **Figure 7:** Relationship of average SO_2 concentrations and normalised gradients a_N^* for the sites
1587 with available data (a) and for the sites with available data excluding UKRO (b).

1588

1589 **Figure 8:** Relationship of average O_3 concentrations and normalised gradients a_N^* .

1590 **Table 1:** Location and data availability of the sites.

Site	Location	Available data	Meteorological data location	Data availability	Reference
UKRU	Harwell Science Centre, Oxford, 80 km W of London, UK (51° 34' 15" N; 1° 19' 31" W)	SMPS (16.6 - 604 nm, 76.5% availability), NO _x , SO ₂ , O ₃ , OC, SO ₄ ²⁻ , gaseous ammonia	On site	2009 - 2015	Charron et al., 2013
UKUB	North Kensington, 4 km W of London city centre, UK (51° 31' 15" N; 0° 12' 48" W)	SMPS (16.6 - 604 nm, 83.3% availability), NO _x , SO ₂ , O ₃ , OC, SO ₄ ²⁻	Heathrow airport	2009 - 2015	Bigi and Harrison, 2010
UKRO	Marylebone Road, London, UK (51° 31' 21" N; 0° 9' 16" W)	SMPS (16.6 - 604 nm, 74.3% availability), NO _x , SO ₂ , O ₃ , OC, SO ₄ ²⁻	Heathrow airport	2009 - 2015	Charron and Harrison, 2003
DENRU	Lille Valby, 25 km W of Copenhagen, (55° 41' 41" N; 12° 7' 7" E) (2008 - 6/2010) Risø, 7 km north of Lille Valby, (55° 38' 40" N; 12° 5' 19" E) (7/2010 - 2017)	DMPS and CPC (5.8 - 700 nm, 68.3% availability), NO _x , SO ₂ , O ₃ , OC, SO ₄ ²⁻	H.C. Ørsted - Institute station	2008 - 2017	Ketzel et al., 2004
DENUB	H.C. Ørsted - Institute, 2 km NE of the city centre, Copenhagen, Denmark (55° 42' 1" N; 12° 33' 41" E)	DMPS and CPC (5.8 - 700 nm, 61.4% availability), NO _x , O ₃	On site	2008 - 2017	Wang et al., 2010
DENRO	H.C. Andersens Boulevard, Copenhagen, Denmark (55° 40' 28" N; 12° 34' 16" E)	DMPS and CPC (5.8 - 700 nm, 65.7% availability), NO _x , SO ₂ , O ₃ , OC, SO ₄ ²⁻	H.C. Ørsted - Institute station	2008 - 2017	Wang et al., 2010
GERRU	Melpitz, 40 km NE of Leipzig, Germany (51° 31' 31.85" N; 12° 26' 40.30" E)	TDMPS with CPC (4.8 - 800 nm, 87.2% availability), OC, SO ₄ ²⁻	On site	2008 - 2011	Birmili et al., 2016
GERUB	Tropos, 3 km NE from the city centre of Leipzig, Germany (51° 21' 9.1" N; 12° 26' 5.1" E)	TDMPS with CPC (3 - 800 nm, 90.4% availability)	On site	2008 - 2011	Birmili et al., 2016
GERRO	Eisenbahnstraße, Leipzig, Germany (51° 20' 43.80" N; 12° 24' 28.35" E)	TDMPS with CPC (4 - 800 nm, 68.3% availability)	Tropos station	2008 - 2011	Birmili et al., 2016
FINRU	Hyytiälä, 250 km N of Helsinki, Finland (61° 50' 50.70" N; 24° 17' 41.20" E)	TDMPS with CPC (3 - 1000 nm, 98.2% availability), NO _x , SO ₂ , O ₃ , VOCs	On site	2008 - 2011 & 2015 - 2018	Aalto et al., 2001
FINUB	Kumpula Campus 4 km N of the city centre, Helsinki, Finland (60° 12' 10.52" N; 24° 57' 40.20" E)	TDMPS with CPC (3.4 - 1000 nm, 99.7% availability)	On site	2008 - 2011 & 2015 - 2018	Järvi et al., 2009
FINRO	Mäkelänkatu street, Helsinki, Finland (60° 11' 47.57" N; 24° 57' 6.01" E)	DMPS (6 - 800 nm, 90.0% availability), NO _x , O ₃	Pasila station and on site	2015 - 2018	Hietikko et al., 2018
SPARU	Montseny, 50 km NNE from Barcelona, Spain (41° 46' 45" N; 2° 21' 29" E)	SMPS (9 - 856 nm, 53.7% availability), NO ₂ , SO ₂ , O ₃	On site	2012 - 2015	Dall'Osto et al., 2013
SPAUB	Palau Reial, Barcelona, Spain (41° 23' 14" N; 2° 6' 56" E)	SMPS (11 - 359 nm, 88.1% availability), NO ₂ , SO ₂ , O ₃	On site	2012 - 2015	Dall'Osto et al., 2012
GRERU	Finokalia, 70 km E of Heraklion, Greece (35° 20' 16.8" N; 25° 40' 8.4" E)	SMPS (8.77 - 849 nm, 85.0% availability), NO ₂ , O ₃ , OC	On site	2012 - 2018	Kalkavouras et al., 2017
GREUB	"Demokritos", 12 km NE from the city centre, Athens, Greece (37° 59' 41.96" N; 23° 48' 57.56" E)	SMPS (10 - 550 nm, 88.0% availability)	On site	2015 - 2018	Mølgaard et al., 2013

Table 2: Frequency (and number), growth and formation rate of class Ia NPF events.

Site	Frequency of NPF events (%)	GR (nm h⁻¹)	J₁₀ (N cm⁻³ s⁻¹)
UKRU	7.0 (160)	3.4*	8.69E-03**
UKUB	7.0 (156)	4.2*	1.42E-02**
UKRO	6.1 (120)	5.5*	3.75E-02**
DENRU	7.9 (176)	3.19	2.57E-02
DENUB	5.8 (116)	3.19	2.40E-02
DENRO	5.4 (117)	4.45	8.07E-02
GERRU	17.1 (164)	4.34	9.18E-02
GERUB	17.5 (169)	4.24	1.02E-01
GERRO	9.0 (62)	5.17	1.38E-01
FINRU	8.7 (190)	2.91	1.19E-02
FINUB	5.0 (110)	2.87	2.49E-02
FINRO	5.1 (49)	3.74	6.94E-02
SPARU	12 (68)	3.87	1.54E-02
SPAUB	13.1 (97)	3.71	2.12E-02
GRERU	6.5 (116)	3.68	4.90E-03
GREUB	8.5 (82)	3.4	4.41E-02

* GR up to 50 nm calculated

** J₁₆ calculated

Table 3: Normalised gradients (non-normalised for growth rate), R^2 and p-values (- for values >0.05) for the relation between meteorological conditions and NPF event variables. Gradients of $R^2 > 0.50$ are in bold.

Downward shortwave solar radiation K_{\downarrow} ($W\ m^{-2}$)										
Site	a_N^* ($W^{-1}\ m^2$)	R^2	p	a_G	R^2	p	a_J^* ($W^{-1}\ m^2$)	R^2	p	Average
UKRU*	1.21E-03	0.94	<0.001	6.53E-05	0.11	-	6.28E-04	0.93	<0.001	443
UKUB*	6.81E-04	0.90	<0.001	-8.26E-05	0.10	-	1.49E-04	0.19	-	448
UKRO*	8.69E-04	0.98	<0.001	-7.75E-06	0.00	-	2.66E-04	0.64	<0.005	464
DENRU	2.22E-03	0.88	<0.001	4.24E-04	0.20	-	1.38E-03	0.64	<0.001	115
DENUB	1.87E-03	0.91	<0.001	1.47E-04	0.03	-	8.98E-04	0.48	<0.01	115
DENRO	2.46E-03	0.95	<0.001	1.27E-04	0.01	-	6.77E-04	0.50	<0.005	117
GERRU	2.87E-03	0.98	<0.001	9.88E-04	0.72	<0.01	1.45E-03	0.81	<0.001	130
GERUB	3.18E-03	0.97	<0.001	7.28E-04	0.51	<0.005	1.53E-03	0.69	<0.001	114
GERRO	2.40E-03	0.95	<0.001	-5.89E-04	0.09	-	9.95E-04	0.59	<0.005	114
FINRU	2.63E-03	0.76	<0.001	1.01E-03	0.57	<0.01	2.04E-03	0.82	<0.001	91.5
FINUB	1.38E-03	0.37	-	1.81E-04	0.08	-	8.99E-04	0.25	-	111
FINRO	1.76E-03	0.59	<0.005	9.15E-04	0.34	<0.005	4.45E-04	0.03	-	114
SPARU	3.46E-04	0.35	<0.05	5.68E-04	0.13	-	1.97E-03	0.74	<0.001	162
SPAUB	5.92E-04	0.58	<0.05	6.98E-04	0.23	-	1.58E-03	0.81	<0.001	180
GRERU	4.10E-04	0.52	<0.001	7.14E-04	0.55	<0.001	-6.30E-04	0.05	-	201
GREUB	3.49E-04	0.31	-	-1.10E-04	0.02	-	8.97E-04	0.34	<0.05	183

* Global solar irradiation measurements in $kJ\ m^{-2}$

Relative Humidity (%)										
Site	a_N^* ($\%^{-1}$)	R^2	p	a_G	R^2	p	a_J^* ($\%^{-1}$)	R^2	p	Average
UKRU	-5.89E-02	0.85	<0.001	1.69E-03	0.02	-	-3.35E-02	0.85	<0.001	79.7
UKUB	-3.42E-02	0.94	<0.001	8.23E-03	0.24	-	-5.66E-03	0.19	-	75.3
UKRO	-5.09E-02	0.85	<0.001	7.03E-03	0.25	-	-1.49E-02	0.46	<0.05	74.5
DENRU	-3.90E-02	0.95	<0.001	9.42E-03	0.74	<0.001	5.45E-04	0.00	-	75.7
DENUB	-3.14E-02	0.94	<0.001	3.64E-03	0.06	-	2.57E-03	0.00	-	75.7
DENRO	-3.64E-02	0.95	<0.001	-1.21E-02	0.22	-	-3.91E-03	0.10	-	75.7
GERRU	-5.08E-02	0.88	<0.001	-1.30E-02	0.72	<0.001	-2.46E-02	0.91	<0.001	81.9
GERUB	-5.35E-02	0.86	<0.001	-6.34E-03	0.67	<0.001	-2.25E-02	0.86	<0.001	78.7
GERRO	-2.83E-02	0.90	<0.001	3.98E-03	0.05	-	-1.72E-02	0.81	<0.001	78.7
FINRU	-4.48E-02	0.94	<0.001	-7.07E-03	0.65	<0.001	-2.16E-02	0.87	<0.001	80.1
FINUB	-5.89E-02	0.95	<0.001	1.04E-02	0.26	-	-6.52E-03	0.18	-	76.5
FINRO	-3.34E-02	0.92	<0.001	-1.47E-03	0.01	-	7.39E-03	0.10	-	71.1
SPARU	-1.54E-02	0.90	<0.001	-4.67E-03	0.08	-	-7.12E-03	0.14	-	66.4
SPAUB	-4.84E-02	0.93	<0.001	2.43E+02	0.50	<0.01	-9.83E-03	0.19	-	69.2
GRERU	-7.72E-03	0.22	-	1.06E-02	0.06	-	-1.83E-01	0.15	-	70.0
GREUB	-1.42E-02	0.62	<0.001	2.83E-03	0.06	-	4.85E-04	0.00	-	60.5

Temperature (°C)										
Site	a_N^* (°C ⁻¹)	R ²	P	a_G	R ²	P	a_J^* (°C ⁻¹)	R ²	P	Average
UKRU	1.10E-01	0.93	<0.001	7.85E-02	0.94	<0.001	8.72E-02	0.84	<0.001	10.6
UKUB	9.04E-02	0.98	<0.001	1.39E-01	0.96	<0.001	6.34E-02	0.73	<0.005	11.8
UKRO	8.22E-02	0.98	<0.001	3.51E-02	0.52	<0.05	4.32E-02	0.44	<0.05	12.1
DENRU	6.68E-02	0.83	<0.001	1.54E-02	0.08	-	6.68E-02	0.92	<0.001	9.80
DENUB	2.50E-02	0.45	<0.05	2.40E-02	0.33	-	3.05E-02	0.45	<0.05	9.82
DENRO	6.64E-02	0.88	<0.001	3.51E-03	0.00	-	2.96E-02	0.58	<0.005	10.0
GERRU	7.27E-02	0.92	<0.001	5.65E-02	0.92	<0.001	5.37E-02	0.93	<0.001	10.3
GERUB	8.20E-02	0.93	<0.001	3.38E-02	0.62	<0.001	4.28E-02	0.54	<0.005	11.1
GERRO	5.08E-02	0.89	<0.001	-3.33E-03	0.00	-	1.61E-02	0.11	-	11.1
FINRU	-2.01E-02	0.17	-	1.13E-01	0.79	<0.001	4.27E-02	0.72	<0.001	4.79
FINUB	-4.21E-03	0.00	-	7.42E-02	0.83	<0.001	1.67E-02	0.28	-	6.52
FINRO	6.24E-02	0.65	<0.005	9.28E-02	0.87	<0.001	-1.09E-02	0.05	-	7.72
SPARU	-2.51E-02	0.41	<0.05	1.23E-01	0.92	<0.001	9.11E-02	0.71	<0.001	13.9
SPAUB	-3.43E-03	0.02	-	6.67E-02	0.66	<0.005	1.18E-02	0.08	-	18.2
GRERU	-4.66E-02	0.75	<0.001	1.74E-01	0.75	<0.001	-9.45E-02	0.47	<0.05	18.2
GREUB	-1.00E-02	0.25	-	4.67E-02	0.62	<0.005	-2.85E-02	0.20	-	17.6

Wind Speed (m s ⁻¹)										
Site	a_N^* (m ⁻¹ s)	R ²	P	a_G	R ²	P	a_J^* (m ⁻¹ s)	R ²	P	Average
UKRU	5.72E-02	0.20	-	-3.04E-02	0.07	-	6.87E-03	0.00	-	3.96
UKUB	1.72E-01	0.87	<0.001	-1.91E-01	0.71	<0.001	3.56E-03	0.00	-	4.16
UKRO	6.34E-02	0.19	-	3.21E-02	0.02	-	7.28E-02	0.45	<0.005	4.14
DENRU	1.08E-01	0.88	<0.001	-2.33E-01	0.74	<0.001	1.28E-01	0.44	<0.01	4.17
DENUB	1.50E-01	0.90	<0.001	-3.33E-02	0.10	-	8.31E-02	0.19	-	4.17
DENRO	1.65E-01	0.89	<0.001	-1.51E-01	0.49	<0.001	9.08E-03	0.00	-	4.16
GERRU	-1.06E-01	0.57	<0.005	-2.26E-01	0.83	<0.001	-5.32E-03	0.00	-	2.58
GERUB	-1.27E-01	0.52	<0.01	-1.41E-01	0.60	<0.005	-3.32E-02	0.04	-	2.33
GERRO	-2.40E-01	0.56	-	-2.54E-01	0.38	-	-1.30E-01	0.22	-	2.33
FINRU	1.62E-01	0.63	<0.005	-1.29E-01	0.16	<0.05	7.99E-02	0.07	-	1.31
FINUB	-3.17E-02	0.08	-	7.26E-02	0.20	<0.05	-9.74E-02	0.17	-	3.43
FINRO	8.62E-02	0.51	<0.05	-1.60E-01	0.32	<0.05	-1.86E-01	0.32	-	4.26
SPARU	-2.20E-02	0.02	-	3.80E-01	0.31	-	5.74E-02	0.02	-	0.94
SPAUB	2.90E-01	0.93	<0.001	7.71E-02	0.24	-	-5.90E-02	0.05	-	2.05
GRERU	4.37E-02	0.54	<0.001	1.01E-01	0.36	<0.005	1.73E-03	0.00	-	6.06
GREUB	-1.13E-01	0.47	<0.01	-1.88E-01	0.50	<0.005	-3.78E-02	0.01	-	1.87

Atmospheric Pressure (mbar)										
Site	a_N^* (mbar ⁻¹)	R ²	P	a_G	R ²	P	a_J^* (mbar ⁻¹)	R ²	P	Average
UKRU	4.26E-02	0.83	<0.005	3.93E-02	0.58	<0.005	2.95E-02	0.47	<0.05	1007.7
UKUB	1.90E-02	0.50	-	1.17E-02	0.05	<0.05	4.16E-03	0.04	-	1011.7
UKRO	6.33E-02	0.95	<0.001	-1.21E-01	0.40	-	-2.98E-02	0.17	-	1012
GERRU	5.10E-02	0.97	-	8.95E-02	0.85	<0.001	2.16E-02	0.21	-	1007.0
GERUB	6.27E-02	0.97	-	4.00E-02	0.76	-	2.00E-02	0.37	<0.05	995.5
GERRO	4.57E-02	0.79	-	-9.61E-02	0.43	-	-2.80E-02	0.21	-	995.5
FINRU	3.46E-02	0.88	<0.001	2.90E-02	0.57	<0.001	1.05E-02	0.14	-	985.1
FINUB	2.61E-02	0.55	<0.005	-3.57E-03	0.02	-	4.38E-03	0.05	-	1004.4
FINRO	4.91E-02	0.70	-	-2.67E-02	0.17	-	1.43E-02	0.26	-	1008.8
SPARU	-2.02E-02	0.09	-	4.79E-02	0.14	-	2.89E-02	0.08	-	939.3
SPAUB	-2.83E-02	0.44	<0.05	1.86E-02	0.08	-	1.68E-02	0.21	-	1006.3
GRERU	6.00E-02	0.46	<0.001	-1.50E-01	0.73	-	8.14E-02	0.33	-	1014.5
GREUB	9.42E-03	0.10	<0.05	-1.00E-01	0.71	-	1.58E-02	0.04	-	1015.7

1605 **Table 4:** Normalised gradients (non-normalised for growth rate), R^2 and p-values (- for values >0.05) for the relation between atmospheric composition variables and NPF event variables. Gradients of $R^2 > 0.50$ are in bold.

SO ₂ (µg m ⁻³)										
Site	a _N * (µg ⁻¹ m ³)	R ²	P	a _G	R ²	P	a _J * (µg ⁻¹ m ³)	R ²	P	Average
UKRU	-1.97E-01	0.38	<0.05	-6.17E-02	0.02	-	3.30E-01	0.06	-	1.64
UKUB	-2.57E-01	0.62	<0.001	1.93E-02	0.00	-	4.18E-01	0.40	-	2.04
UKRO	-1.03E-01	0.82	<0.001	6.90E-02	0.34	<0.01	8.43E-02	0.77	<0.001	7.46
DENRU	-9.77E-01	0.53	<0.05	2.84E+00	0.37	-	4.38E-01	0.09	-	0.52
DENRO	-4.20E-01	0.91	<0.001	6.42E-01	0.54	<0.005	5.66E-01	0.62	<0.001	0.97
FINRU	-5.66E-01	0.05	-	-1.42E+00	0.19	-	-6.30E-02	0.00	-	0.09
SPARU	-3.62E-01	0.74	<0.001	-1.33E-01	0.02	-	-3.55E-02	0.01	-	0.95
SPAUB	-2.93E-02	0.04	-	4.12E-01	0.59	-	1.07E-01	0.29	-	1.99

NO _x or NO ₂ (ppb)										
Site	a _N * (ppb ⁻¹)	R ²	P	a _G	R ²	P	a _J * (ppb ⁻¹)	R ²	P	Average
UKRU	-4.99E-02	0.67	<0.005	4.52E-02	0.58	<0.05	-4.51E-02	0.70	<0.005	11.7
UKUB	-8.75E-03	0.83	<0.001	-3.97E-04	0.00	-	-1.09E-02	0.43	<0.05	53.6
UKRO	-3.22E-03	0.72	<0.001	1.44E-03	0.39	<0.05	2.19E-03	0.66	<0.001	299
DENRU	-9.41E-02	0.43	<0.005	-4.89E-03	0.00	<0.001	-6.47E-02	0.55	<0.01	5.42
DENUB	-4.99E-02	0.68	<0.001	2.85E-02	0.26	-	8.55E-04	0.00	-	10.5
DENRO	-5.10E-03	0.75	<0.001	1.10E-02	0.69	<0.001	8.33E-03	0.88	<0.001	68.5
FINRU	-7.27E-01	0.54	<0.001	-2.74E-01	0.11	-	1.95E-01	0.05	-	0.72
FINRO	-6.24E-03	0.68	<0.001	1.70E-03	0.12	-	3.25E-03	0.03	-	88.1
SPARU*	-1.53E-02	0.05	-	2.54E-02	0.01	-	1.25E-01	0.21	-	3.26
SPAUB*	-2.59E-02	0.62	<0.005	2.23E-02	0.70	<0.001	2.57E-03	0.01	-	31.4
GRERU*	3.01E-01	0.19	-	-1.40E+00	0.75	<0.001	5.23E-01	0.13	-	0.52

1610

* NO₂ measurements

O ₃ (ppb)										
Site	a _N * (ppb ⁻¹)	R ²	p	a _G	R ²	p	a _J * (ppb ⁻¹)	R ²	p	Average
UKRU	2.27E-02	0.88	<0.001	-4.89E-02	0.53	<0.005	-3.53E-03	0.01	-	54.4
UKUB	1.37E-02	0.87	<0.001	-3.45E-02	0.68	<0.001	-5.95E-03	0.05	-	39.3
UKRO	7.46E-02	0.95	<0.001	-1.06E-02	0.09	-	-2.44E-02	0.63	<0.005	16.2
DENRU	4.97E-02	0.92	<0.001	-1.32E-02	0.15	-	1.23E-02	0.08	-	30.1
DENUB	5.85E-02	0.84	<0.001	-1.69E-02	0.58	-	2.77E-02	0.32	<0.05	28.2
DENRO	6.42E-02	0.51	<0.05	1.39E-02	0.03	-	3.24E-02	0.91	<0.05	31.1
FINRU	6.76E-02	0.77	<0.05	-4.23E-02	0.60	-	3.92E-02	0.37	<0.05	27.4
FINRO	2.38E-02	0.91	<0.001	6.11E-03	0.24	-	-1.83E-02	0.29	-	37.1
SPARU	1.57E-02	0.02	-	4.34E-02	0.11	-	1.31E-02	0.31	-	75.9
SPAUB	7.99E-03	0.38	<0.05	-5.83E-03	0.30	-	-1.13E-03	0.01	-	54.9
GRERU	7.55E-03	0.04	-	3.68E-02	0.17	-	-3.01E-02	0.15	-	49.5

Particulate Organic Carbon (µg m ⁻³)										
Site	a _N * (µg ⁻¹ m ³)	R ²	p	a _G	R ²	p	a _J * (µg ⁻¹ m ³)	R ²	p	Average
UKRU	-3.30E-02	0.00	-	1.13E+00	0.42	<0.005	2.13E-01	0.16	-	1.96
UKUB	-2.76E-01	0.59	<0.005	6.63E-01	0.58	<0.05	2.19E-01	0.55	<0.05	3.63
UKRO	-3.78E-01	0.89	<0.001	8.12E-01	0.57	<0.005	4.60E-01	0.75	<0.001	6.24
DENRU	-4.44E-01	0.75	<0.001	2.24E-01	0.11	-	-3.17E-01	0.68	<0.01	1.48
DENRO	-7.80E-02	0.11	-	1.10E+00	0.77	<0.005	4.02E-01	0.81	<0.005	2.59
GERRU	-1.26E-01	0.24	-	1.35E-01	0.09	-	3.14E-02	0.03	-	2.18
FINRU	2.27E-02	0.00	-	3.39E-01	0.60	<0.005	-3.46E-01	0.16	-	1.78
GRERU	-2.08E-01	0.11	-	7.87E-01	0.41	<0.05	8.94E-01	0.11	-	1.58

Sulphate (µg m ⁻³)										
Site	a _N * (µg ⁻¹ m ³)	R ²	p	a _G	R ²	p	a _J * (µg ⁻¹ m ³)	R ²	p	Average
UKRU ¹	-2.62E-01	0.57	<0.001	7.34E-01	0.77	<0.001	7.99E-01	0.44	<0.05	1.97
UKUB ¹	-3.57E-01	0.89	<0.001	9.28E-01	0.44	<0.01	9.72E-01	0.16	-	1.58
UKRO ¹	-6.05E-02	0.24	-	3.04E-01	0.34	<0.05	-6.22E-02	0.04	-	1.98
DENRU ²	-7.81E-01	0.34	<0.05	1.02E+00	0.60	<0.05	-1.03E+00	0.63	<0.01	0.52
DENRO ²	-8.23E-01	0.28	-	1.99E+00	0.22	-	2.82E-01	0.12	-	0.55
GERRU ¹	-3.37E-02	0.00	-	5.89E-01	0.11	-	-4.89E-02	0.01	-	0.92
FINRU ³	-1.18E+00	0.65	<0.001	2.35E-01	0.09	-	-2.53E-01	0.17	-	1.02

¹ Measurements in PM₁₀

² Measurements in PM_{2.5}

³ Measurements in PM₁

Condensation Sink (s^{-1})										
Site	a_N^* (s)	R^2	P	a_G	R^2	P	a_J^* (s)	R^2	P	Average
UKRU	-2.28E+02	0.72	<0.001	2.64E+02	0.60	<0.001	7.58E+01	0.22	-	3.38E-03
UKUB	-1.66E+02	0.78	<0.001	2.49E+02	0.41	<0.05	1.73E+02	0.35	<0.05	7.41E-03
UKRO	-4.03E+01	0.75	<0.001	2.33E+01	0.18	-	8.94E+01	0.91	<0.001	2.12E-02
DENRU	-4.48E+01	0.91	<0.001	6.90E+01	0.49	<0.05	5.37E+01	0.24	-	9.46E-03
DENUB	-3.78E+01	0.75	<0.001	3.58E+01	0.25	-	1.55E+01	0.56	<0.005	1.42E-02
DENRO	-1.06E+01	0.73	<0.001	2.53E+01	0.56	<0.005	2.72E+01	0.79	<0.001	3.10E-02
GERRU	1.54E+02	0.86	<0.001	1.33E+02	0.56	<0.001	6.67E+01	0.63	<0.001	7.02E-03
GERUB	3.59E+01	0.56	<0.005	3.63E+01	0.17	-	4.74E+01	0.75	<0.001	9.11E-03
GERRO	3.89E+01	0.22	<0.05	-2.21E+01	0.03	<0.005	3.54E+01	0.45	<0.005	1.20E-02
FINRU	-1.80E+02	0.59	<0.005	4.01E+02	0.74	<0.001	4.98E+01	0.10	-	2.32E-03
FINUB	-1.51E+02	0.63	<0.005	8.14E+01	0.31	-	2.01E+02	0.41	<0.05	6.34E-03
FINRO	-6.99E+01	0.77	<0.001	-1.56E+01	0.05	-	2.42E+02	0.83	<0.001	8.96E-03
SPARU	-2.15E+02	0.65	<0.005	1.86E+01	0.00	-	8.60E+01	0.47	<0.05	5.49E-03
SPAUB	-1.18E+02	0.65	<0.005	3.74E+01	0.38	<0.05	9.51E+01	0.52	<0.01	1.00E-02
GRERU	4.33E+00	0.00	-	2.86E+02	0.70	<0.001	1.77E+02	0.56	<0.005	4.66E-03
GREUB	1.64E+02	0.65	<0.001	9.31E+01	0.28	<0.05	1.73E+02	0.83	<0.001	7.55E-03

1620

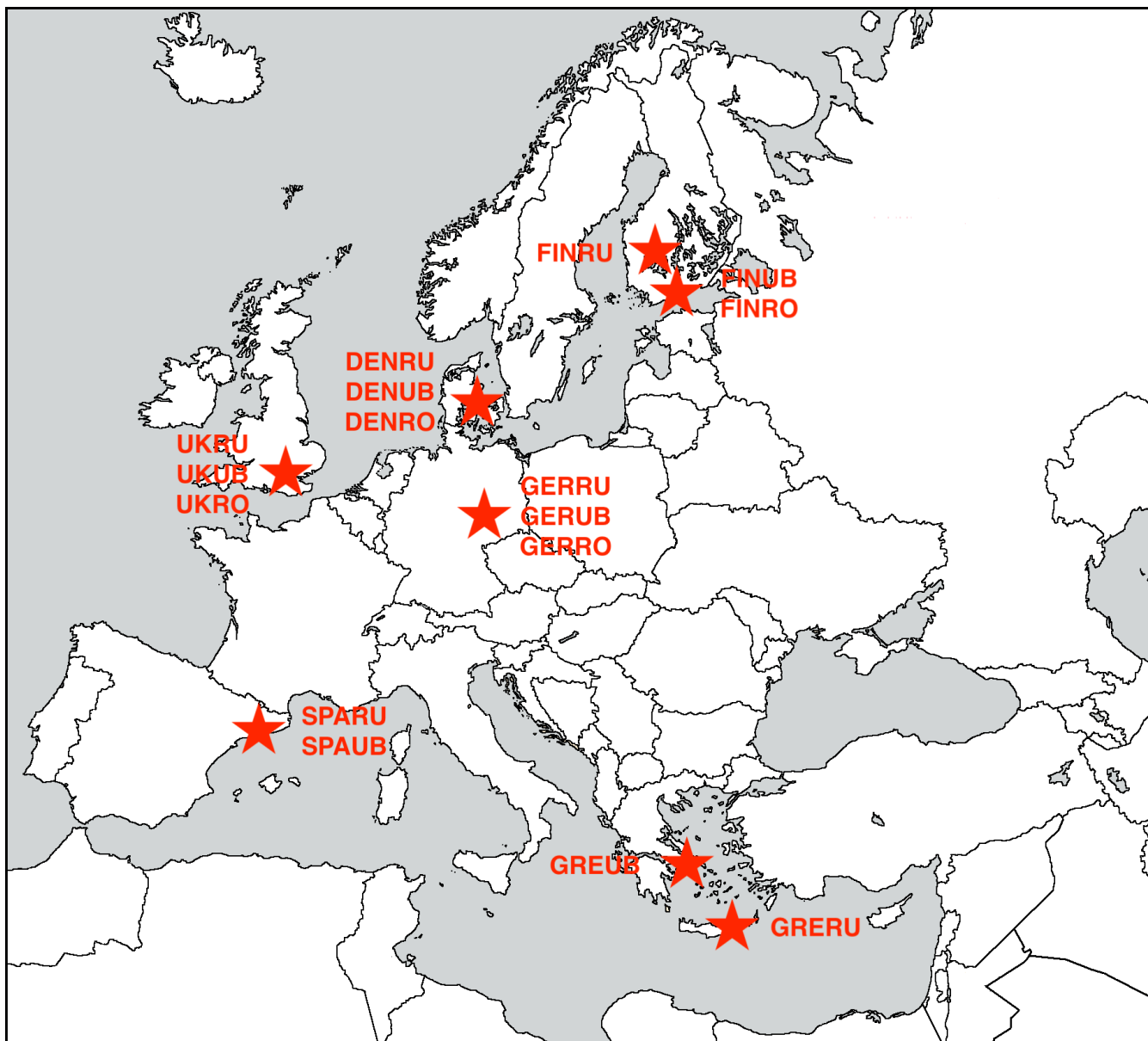


Figure 1: Map of the sites of the present study.

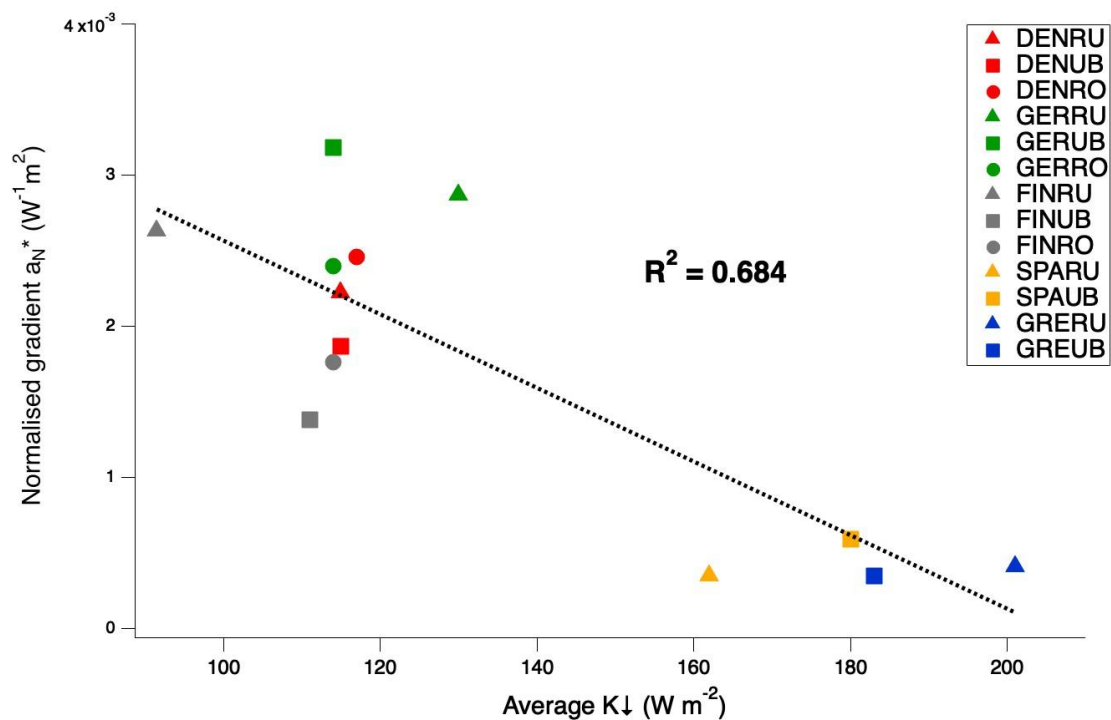


Figure 2: Relationship of average downward incoming solar radiation (K_{\downarrow}) and normalised gradients a_N^* .

1630

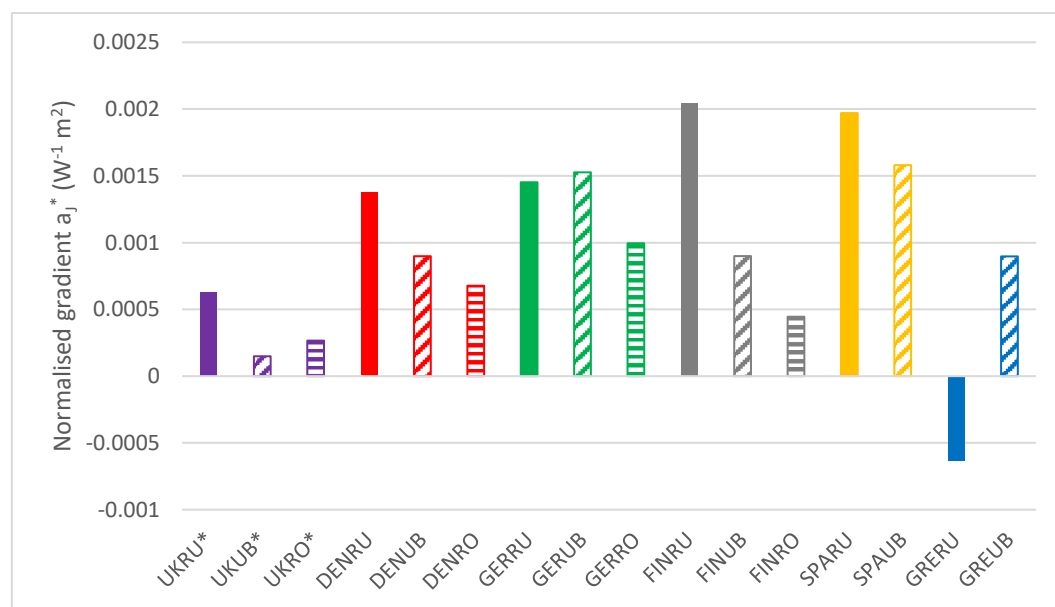
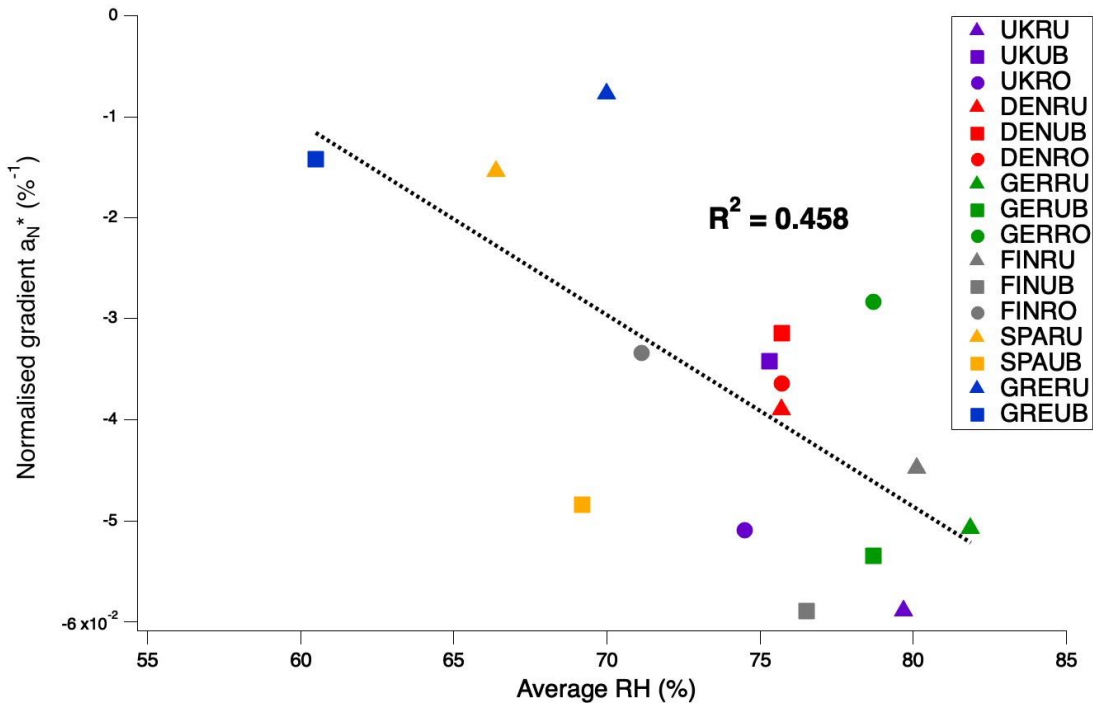


Figure 3: Normalised slopes a_j^* for K_{\downarrow} (*UK sites are calculated with solar irradiance).



1635 **Figure 4:** Relationship of average relative humidity and normalised gradients a_N^* .

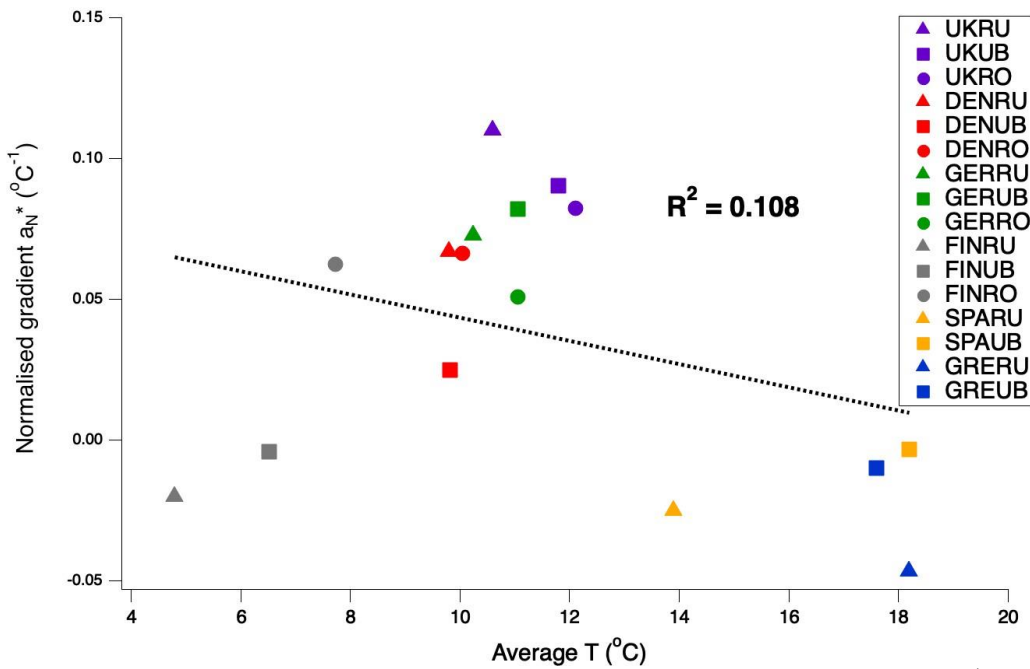


Figure 5: Relationship of average temperature and normalised gradients a_N^* .

1640

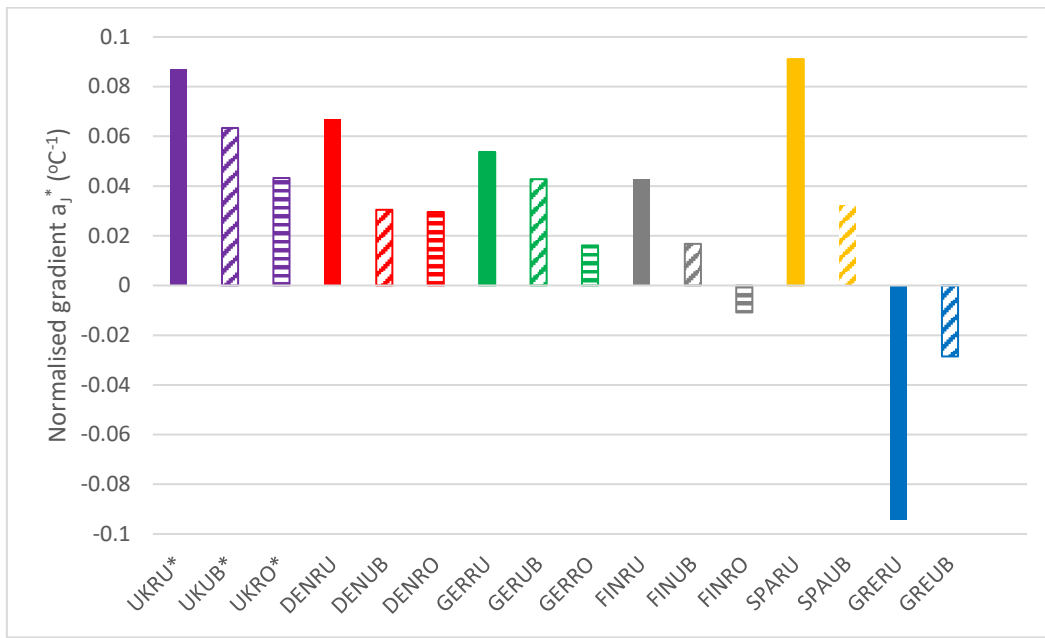


Figure 6: Normalised gradients a_j^* for temperature.

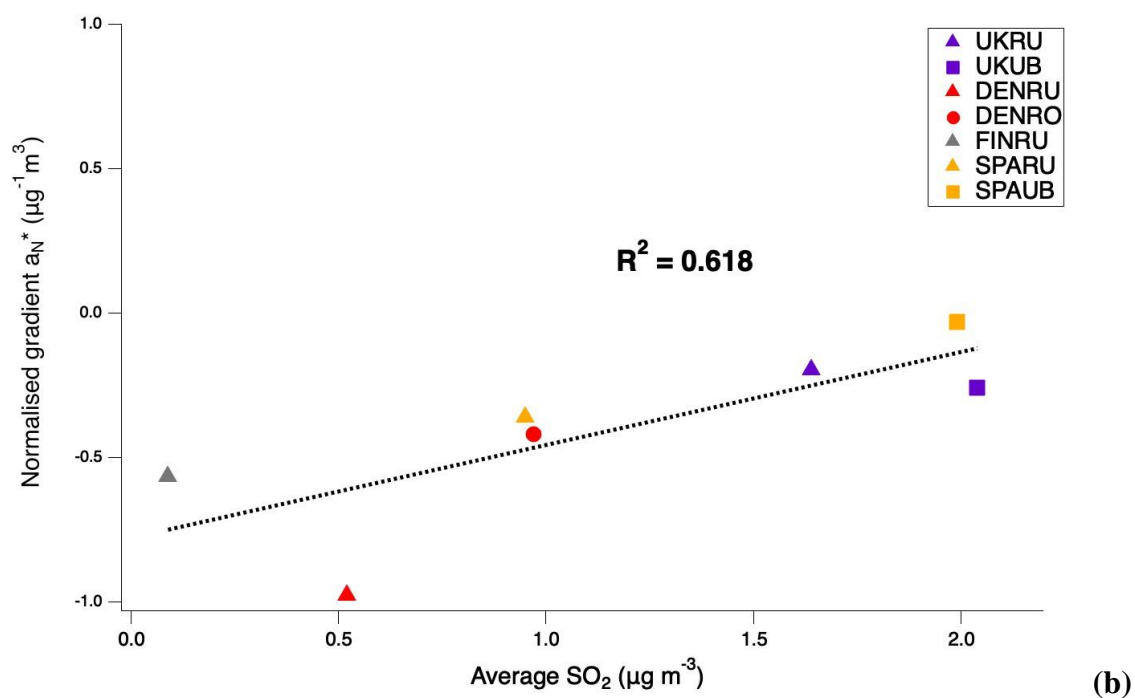
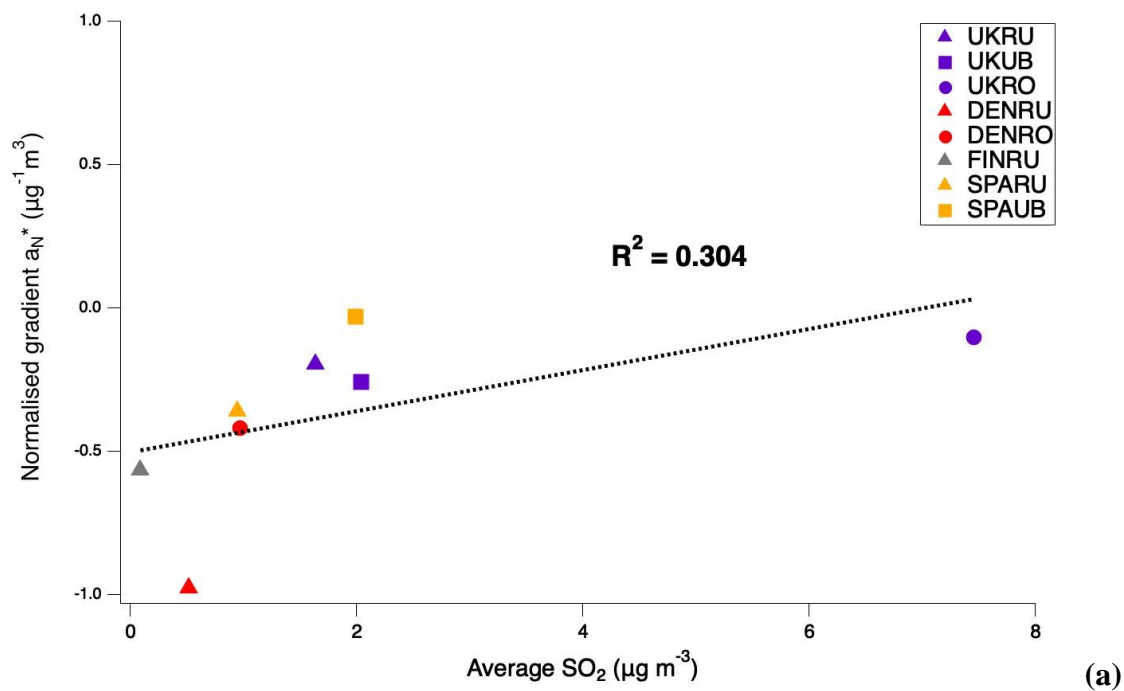
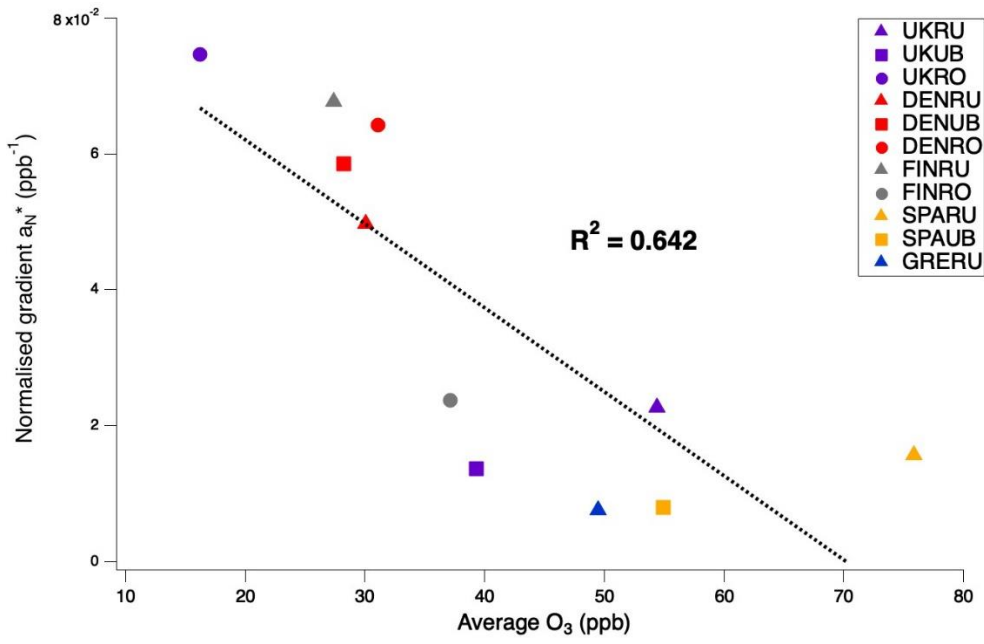


Figure 7: Relationship of average SO_2 concentrations and normalized gradients a_N^* for the sites with available data (a) and for the sites with available data excluding UKRO (b).



1650 **Figure 8:** Relationship of average O₃ concentrations and normalised gradients a_N*.